Research

New Phytologist

Argonaute7 (AGO7) optimizes arbuscular mycorrhizal fungal associations and enhances competitive growth in *Nicotiana attenuata*

Maitree Pradhan, Ian T. Baldwin and Shree P. Pandey

Department of Molecular Ecology, Max Planck Institute for Chemical Ecology, Jena, 07745, Germany

Authors for correspondence:
Ian T. Baldwin
Email: baldwin@ice.mpg.de

Shree P. Pandey
Email: shreeppandey@gmail.com

Received: *23 March 2023*
Accepted: *2 July 2023*

New Phytologist (2023) **240:** 382–398
doi: 10.1111/nph.19155

Key words: AGO7, arbuscular mycorrhizal fungi (AMF), biological function, competition, field studies, miRNA, *Nicotiana attenuata*.

Summary

- Plants interact with arbuscular mycorrhizal fungi (AMF) and in doing so, change transcript levels of many miRNAs and their targets. However, the identity of an Argonaute (AGO) that modulates this interaction remains unknown, including in *Nicotiana attenuata*.
- We examined how the silencing of NaAGO1/2/4/7/and 10 by RNAi influenced plant-competitive ability under low-P conditions when they interact with AMF. Furthermore, the roles of seven miRNAs, predicted to regulate signaling and phosphate homeostasis, were evaluated by transient overexpression.
- Only *NaAGO7* silencing by RNAi (ir*AGO7*) significantly reduced the competitive ability under P-limited conditions, without changes in leaf or root development, or juvenile-to-adult phase transitions. In plants growing competitively in the glasshouse, ir*AGO7* roots were over-colonized with AMF, but they accumulated significantly less phosphate and the expression of their AMF-specific transporters was deregulated. Furthermore, the AMF-induced miRNA levels were inversely regulated with the abundance of their target transcripts. miRNA overexpression consistently decreased plant fitness, with four of seven-tested miRNAs reducing mycorrhization rates, and two increasing mycorrhization rates. Overexpression of Na-miR473 and Na-miRNA-PN59 downregulated targets in GA, ethylene, and fatty acid metabolism pathways.
- We infer that AGO7 optimizes competitive ability and colonization by regulating miRNA levels and signaling pathways during a plant's interaction with AMF.

Introduction

Small RNAs (smRNAs) regulate many aspects of a plant's phenotypic plasticity while they respond to changes in their abiotic and biotic environments (Axtell, 2013; Borges & Martienssen, 2015; Brant & Budak, 2018; Manavella *et al.*, 2019; Song *et al.*, 2019). All characterized smRNA processes engage an Argonaute (AGO), which functions as a direct binding partner of the smRNAs during the formation of the RNA-induced silencing complex (RISC). AGOs facilitate endonucleolytic cleavage of transcripts, translational repression, RNA-directed DNA methylation, synthesis of secondary small interfering RNAs (siRNAs), Dicer (DCL)-independent pre-microRNA (miRNA) synthesis, and co-transcriptional regulation of miRNA gene expression (Meister, 2013; Fang & Qi, 2016; Carbonell, 2017). As a consequence, AGOs are regarded as the 'effectors' of the smRNA machinery.

The size of the *AGO* families in flowering plants varies by taxa: 10 in Arabidopsis and 19 in rice, whereas the genomes of *Chlamydomonas* (algae) and *Physcomitrella* (moss) contain three and six *AGO*s, respectively. Plant *AGO*s are classified into four major classes (Singh *et al.*, 2015): AGO1/10 (class I), AGO5 (class II), AGO2/3/7 (class III), and AGO4/6/8/9 (class IV). The expansion of the AGO family suggests functional diversification during the evolution of specialized smRNA pathways (Carbonell, 2017; Pradhan *et al.*, 2017); however, biological roles for all AGOs remain to be fully elucidated. While members of class I and class IV AGOs are comparatively well characterized, the functions of class III AGOs (AGO2/3/7) have only been studied in a limited set of species. In Arabidopsis, AGO2 is primarily involved in viral resistance; AtAGO3, while closely related to AtAGO2, remains functionally uncharacterized. AtAGO7 mediates juvenile-to-adult phase transitions and leaf morphogenesis (Hunter *et al.*, 2003; Xu *et al.*, 2006; Fang & Qi, 2016; Carbonell, 2017). AtAGO7 preferentially associates with miR390 and is involved in the processing of 21 nt smRNAs (Cuperus *et al.*, 2009). AtAGO7 binds to miR390 and is required for the biogenesis of ta-siRNAs (Montgomery *et al.*, 2008; Jouannet *et al.*, 2012). The functions of AGO7 in leaf development and ta-siRNA biogenesis are also reported from maize and rice (Nagasaki *et al.*, 2007; Douglas *et al.*, 2010). In the ecological model species, *Nicotiana attenuata*, in which several components of smRNA machinery are well established (Pandey & Baldwin, 2007, 2008; Pandey *et al.*, 2008; Bozorov *et al.*, 2012b; Pradhan *et al.*, 2017, 2020; Navarro-Quezada *et al.*, 2020), the biological

function of NaAGO7 remains unknown. The aim of this study was to address this knowledge gap.

Nicotiana attenuata (coyote tobacco) is an annual tobacco, native to southwestern North America that germinates from long-lived seed banks in post-fire environments to form monocultures (Baldwin & Morse, 1994). The *N. attenuata* genome encodes AGOs homologous to *AGO1* (NaAGO1a, b, c; class I), *AGO2* (class III), *AGO4* (NaAGO4a, b; class IV), *AGO5* (class II), *AGO7* (class III), *AGO8* (class IV), *AGO9* (class I), and *AGO10* (class I) (Singh *et al.*, 2015; Pradhan *et al.*, 2017). Loss-of-function studies have helped to define the biological functions of AGOs of classes I (NaAGO1) and IV (NaAGO4 and NaAGO8). Specifically, the function of AGO1 in development, as reported from many species, is conserved in *N. attenuata* (Pradhan *et al.*, 2017); NaAGO8 modulates *N. attenuata*'s direct defenses induced in response to attack from herbivores (Pradhan *et al.*, 2017) and NaAGO4 (Pradhan *et al.*, 2020) mediates resistance to wilt-like fungal diseases (Schuck *et al.*, 2014; Santhanam *et al.*, 2015).

Nicotiana attenuata also interacts with arbuscular mycorrhizal fungi (AMF), which under glasshouse conditions can produce variable fitness outcomes under P-limited growing conditions (Wang *et al.*, 2018a), but in natural habitats, plants impaired in their ability to associate with AMF (Groten *et al.*, 2015) are commonly outcompeted by isogenic plants that can associate with AMF (Wang *et al.*, 2018a). Marked by distinct stages, root colonization by AMF starts with a pre-symbiotic phase during the first 1–3 d (Gutjahr *et al.*, 2009; Pimprikar & Gutjahr, 2018). During the later stages of colonization, roots are populated with hyphae, vesicles, and arbuscules of different stages of development. The AMF symbiosis is based on the exchange of inorganic phosphorous (P_i), other nutrients and water supplied by the fungus, in exchange for 4–20% of the plant's net photosynthetic carbon fixation (Johnson *et al.*, 1997). This process reprograms the accumulation of transporters (like PT4), whose expressions are tightly and temporally regulated by transcription factors like RAM1 (Pimprikar & Gutjahr, 2018). Phytohormones, in particular auxin, GA, ethylene (ET) signaling, and fatty acid metabolism play important roles in AMF colonization (Choi *et al.*, 2018; Müller & Harrison, 2019).

Phytohormones interact with other factors such as peptides, phosphate signaling pathways, and miRNAs to form a complex signal transduction network, which integrates AMF symbiosis and the P-status of the plant (Müller & Harrison, 2019). miRNAs regulate their targets in a highly sequence-specific manner, which involves an AGO effector (Meister, 2013; Fang & Qi, 2016; Carbonell, 2017). Furthermore, AGOs can influence miRNA accumulations, regulate phytohormone signaling pathways, and modulate the expression of specific target genes by miRNAs in a highly stimulus-dependent manner (Pradhan *et al.*, 2017, 2020).

Whether AGOs are involved in a plant's interactions with AMF has not been directly studied, but smRNAs clearly are reprogrammed during AMF colonization (Wu *et al.*, 2016; Pandey *et al.*, 2018; Song *et al.*, 2018; Silvestri *et al.*, 2019). The roles of miR171a, b and h, miR396, and miR393 (Couzigou & Combier, 2016) have been associated with AMF colonization. In addition, several families of miRNAs, such as miR399, are known to regulate phosphate homeostasis/phosphorous deficiency signaling (Kuo & Chiou, 2011; Wang *et al.*, 2018a); these are likely engaged during AMF colonization, but this functional inference remains untested. Although *N. attenuata*–AMF interactions entail large changes in the root miRNome (Pandey *et al.*, 2018), the specific AGO effectors that mediate this process remain unknown.

We hypothesize that plant–AMF interactions could recruit a specific AGO effector that helps *N. attenuata* maximize its Darwinian fitness in nature. Here, we examined the biological function of *N. attenuata*'s *AGO7*, evaluated AGO7-dependent changes in miRNA abundances, and analyzed the role of AGO7-regulated miRNAs in AMF root colonization, plant fitness, and signaling processes.

Materials and Methods

Plant material and glasshouse growth conditions

Two independent transgenic ir*AGO7* lines (inverted-repeat silenced *AGO7*; A-13-018-8-4 and A-13-017-2-2) did not show any significant differences among each other (Pradhan *et al.*, 2017). Therefore, we randomly selected line A-13-018-8-4 for the experiments presented here. Seeds of the 31st generation wild-type plant (WT) *N. attenuata* Torr. Ex Watts, and all the transgenic plants (ir*AGO1* (A-12–866-1-5), ir*AGO2* (A-12–845-2-8), ir*AGO4* (A-13-021-2-6), ir*AGO7* (A-13-018-8-4), and ir*AGO10* (A-13-025-6-7)) were grown and maintained as described previously (Krügel *et al.*, 2002; Halitschke *et al.*, 2003; Onkokesung *et al.*, 2012) and in Supporting Information Methods S1.

For the glasshouse experiments with AMF, living inoculum (*R. irregularis*, Biomyc Vital, www.biomyc.de, inoculated plants) was used (details in Methods S1). Plants were fertilized every second day with a low phosphate (P) hydroponic solution (Groten *et al.*, 2015; Wang *et al.*, 2018a) as detailed in Methods S1. A WT plant was paired with a size-matched irAGO7 plant in the same pot to force the two genotypes to compete for resources (Pandey *et al.*, 2008). Plant performance was evaluated, samples were harvested and processed, as detailed in Methods S1.

Blumenol analysis and microscopic observations for estimating host–AMF interaction

11-Carboxyblumenol-C-glucoside (blumenol-C) is a reliable quantitative marker for root colonization of AMF and was quantified as previously described (Wang *et al.*, 2018a). Samples were extracted with 80% MeOH and analyzed with a ultra-high-performance liquid chromatography (Methods S1). To determine the fungal colonization rates and mycorrhizal structures, root samples were stained, analyzed, and quantified by microscopy using with Trypan blue and WGA-fluorescein staining (Methods S1; Brundrett *et al.*, 1984; McGonigle *et al.*, 1990).

RNA extraction and quantitative real-time PCR

For miRNA- and mRNA quantifications, qPCR assays were performed (Methods S1; primer sequences are provided in Table S1).

Total RNA was extracted from roots using the lithium chloride method (Kistner & Matamoros, 2005; Pradhan *et al.*, 2017). Specific miRNA sequences were from Pandey *et al.* (2018); miScript SYBR Green PCR kit was used for miRNA-qPCRs. For mRNA quantification, qPCR assays were performed with gene-specific primers on cDNA templates (Methods S1). The 5S rRNA and the sulfite reductase (Na*ECI*) genes were used as endogenous references for miRNAs and mRNAs, respectively. The $2^{-\Delta\Delta CT}$ method was used for data analysis (Bubner *et al.*, 2004; Bubner & Baldwin, 2004; Pandey & Baldwin, 2007; Bozorov *et al.*, 2012a).

Field experiments

All the field experiments were conducted at the Lytle Ranch Preserve (the Great Basin Desert of Southwestern Utah, USA; latitude 37.146, longitude 114.020) in two consecutive years: 2018 and 2019. Transgenic plants were released under APHIS importation and release permits (18-054-101r and 18-282-103r). Planting and data recording are detailed in Methods S1. Experiments were terminated after 8 wk by uprooting the plants as plants started to produce seed capsules, which were removed by hand before maturation, to meet the regulatory requirements of the field releases.

Statistical analysis

Data were analyzed using OriginLab 2016 software. Paired *t*-tests were used for field experiments and ANOVA (one-way and repeated measures) were used in glasshouse studies (Methods S1).

Transient overexpression of Na-miRNAs

Na-miRNAs were transiently overexpressed. Steps of vector construction are detailed in Methods S1; information on relevant sequences are provided in Table S2. Empty vector (EV) constructs were used as controls, and 10–12 biological replicates (plants) were independently inoculated with each construct. Plants overexpressing individual miRNAs and EV controls were grown in 1 l pots in a growth chamber under P-limited conditions with AMF (Methods S1). Growth and fitness parameters were recorded weekly until harvest. AMF colonization was monitored at 6 and 8 wk by analyzing leaf blumenol-C contents. Overexpression was quantified in individual plants with the help of the miRNA-qPCR assays (Methods S1).

Results

NaAGO7-silenced plants are strongly impaired in competitive growth but not in their resistance to pathogens or herbivores in nature

Nicotiana attenuata genome contains an AGO7 homolog, whose expression was silenced (4- to 10-fold) by generating inverted-repeat stable transformants (irAGO7), as previously described in Pradhan *et al.* (2017). Our overarching objective was to determine NaAGO7's biological function. To robustly evaluate this, we planted ir*AGO7* plants into the natural habitat of *N. attenuata* in field plots in the Great Basin Desert. We grew ir*AGO7* and WT pairs in close proximity (20–30 cm; Fig. 1) and assessed their susceptibility to attack from the natural herbivore community as well as their growth and reproductive performance (Pandey *et al.*, 2008). To evaluate *AGO7*'s possible role in resistance against natural pathogens, ir*AGO7*-WT pairs were also planted in an *Alternaria–Fusarium*-infected field plot (Pradhan *et al.*, 2020): ir*AGO7* and WT plants suffered similar mortality rates that could be attributed to fungal infection (Fig. S1a). ir*AGO7* plants were also indistinguishable from the WT neighbors in their ability to defend themselves against natural herbivores (similar total canopy areas damaged; Fig. S1a). From these results, we infer that the loss of Na*AGO7* function does not affect disease resistance or herbivore resistance in nature.

However, ir*AGO7* plants were consistently outcompeted by their WT neighbors as revealed by measures of their growth and reproductive performance, despite being planted as size-matched seedling pairs (Fig. 1). WT plants started to elongate around the 4th wk and stalk lengths of ir*AGO7* plants were significantly shorter than those of WT plants at the end of 4 wk (Fig. 1). Overall, ir*AGO7* plants continued to lag behind their WT counterparts even at the end of 8 wk (Fig. 1). Although we could not estimate lifetime fitness as mature seed capsule production (to prevent release of transgenic seeds in nature), ir*AGO7* plants were clearly impaired in their reproductive output: WT plants started to flower 1 wk earlier than did their ir*AGO7* competitors, and produced significantly more flowers (Fig. 1). After 8 wk, WT plants had produced, on an average, 4–5 seed capsules per plant, while ir*AGO7* plants had not produced any. The biomass of ir*AGO7* plants was significantly lower than that of WT plants at the end of 8 wk (Fig. 1).

Furthermore, we estimated the AMF colonization of the WT and ir*AGO7* plant pairs by measuring blumenol-C levels in the leaves of reproductively mature plants (Wang *et al.*, 2018a). The overall average blumenol-C contents of WT and ir*AGO7* plants were similar (Fig. S1b). At the same time, we noticed that the blumenol-C content of the field-grown plants was strikingly lower than those previously observed for the glasshouse-grown plants (Wang *et al.*, 2018a; Pradhan *et al.*, 2021). WT plants displayed a strong positive correlation between their blumenol-C contents and their reproductive output (flower numbers; Fig. S1b). This correlation between the blumenol-C content and plant reproductive output was not observed in ir*AGO7* plants (Fig. S1b). When we normalized the reproductive output as a function of blumenol-C content, we found that WT plants produced nearly 1.8 times more flowers per unit of blumenol-C than ir*AGO7* plants (Fig. S1b).

From the field observations, we infer that AGO7 silencing reduces the ability of *N. attenuata* plants to compete with conspecifics in natural environments.

Silencing *AGO7* does not affect plant development, juvenile-to-adult transitions, or fitness under resource-rich conditions

Studies in Arabidopsis identified a function for *AGO7* in juvenile-to-adult phase changes and in leaf morphogenesis (Hunter

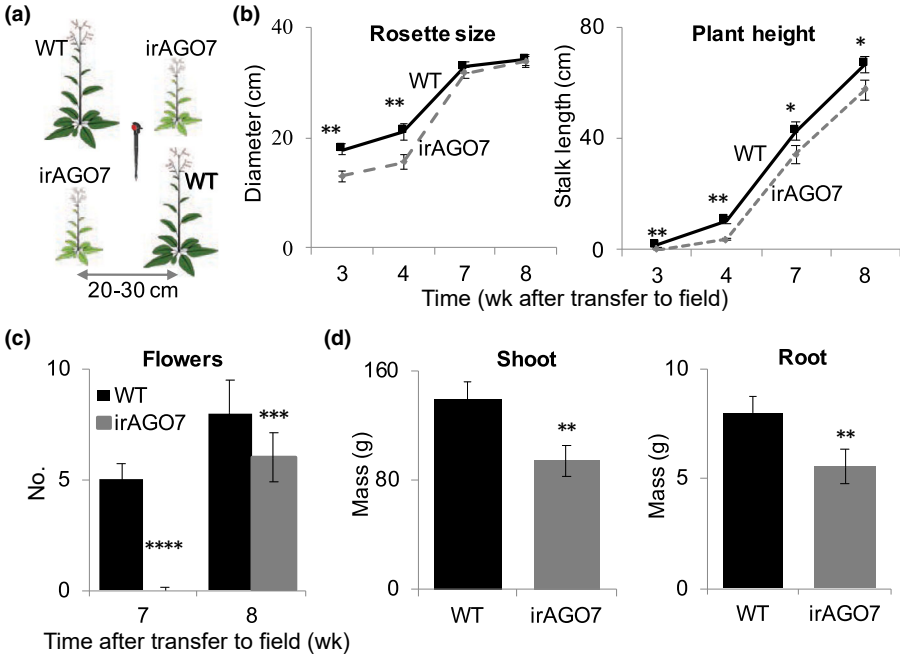

Fig. 1 When planted as competing pairs into a field plots in the plant's native habitat, *AGO7*-silenced *Nicotiana attenuata* plants grow more slowly and produce fewer fitness correlates than initially size-matched wild type (WT) plants. (a) Planting was done in a paired design depicted by the cartoon, where plants were 20–30 cm apart (pin in the middle indicates an irrigation dripper). The two genotypes did not differ in the damage received from the native herbivore community or their mortality due to a fungal wilt disease (Supporting Information Fig. S1). (b) Their rosette diameters and stalk heights were significantly smaller (paired *t*-test, *t*-value = 0.013 and 0.0021 for 3 wk and four rosette diameters; *t*-value = 0.004, 0.01, 0.052 and 0.048 for stalk heights at 3, 4, 7, and 8 wk). Values presented are means ± SD, number of biological replicates (n) = 25 per genotype, * and ** significant differences from WT at $P \leq 0.05$ and $P \leq 0.01$, respectively. (c) ir*AGO7* plants produced significantly fewer flowers than WT ($n = 27$, error bars correspond to SD; **** and *** signify significant differences from WT at $P \leq 0.001$ and 0.005, respectively). (d) Fresh shoot and root biomass of ir*AGO7* plants at the end of the experiment (8 wk post transfer to field plot) were significantly lower than those of WT (paired *t*-test, *t*-value = 0.012 for shoot biomass and 0.013 for root biomass, $n = 23$; errors bars refer to SD).

et al., 2003; Xu *et al.*, 2006; Fang & Qi, 2016; Carbonell, 2017). Such functions were also reported from maize and rice (Nagasaki *et al.*, 2007; Douglas *et al.*, 2010). However, *N. attenuata* ir*AGO7* plants did not exhibit any noticeable change in development under standard growth conditions when resources were not limiting (Fig. 2a; plants were grown singly, in 1 l pot, in soil with a full fertilizer regime; Methods S1). The rosettes of ir*AGO7* and WT plants grew similarly and transitioned to the elongation stage together (Fig. 2a). No significant differences in plant height/stalk length were found between WT and ir*AGO7* plants (Fig. 2a). Furthermore, ir*AGO7* and WT plants produced similar numbers of leaves with similar chlorophyll contents (Fig. S2). Furthermore, we did not find any significant differences in root phenotypes, such as in root length or lateral root numbers, in the two genotypes (Fig. S2). Moreover, no difference in reproductive performance between ir*AGO7* and WT plants was found as both genotypes produced similar numbers of seed capsules and biomass (Fig. 2a). From these data, we infer that silencing Na*AGO7* does not affect *N. attenuata*'s development.

AGO7-silenced plants show reduced growth and fitness under P-limited competitive conditions with AMF inoculation

When initially size-matched ir*AGO7* and WT plants were grown together in the same pot under resource-rich conditions (full fertilizer regimes; without AMF inoculum), no differences in growth or fitness were observed between the two genotypes (Fig. 2b). When grown in the same competitive setup but under phosphate- (P-) limited conditions (10% and 25% of the regular P-levels at rosette and elongation stages, respectively) with AMF inoculum, as previously described (Pandey *et al.*, 2018; Wang *et al.*, 2018a), the rosettes of WT and ir*AGO7* plants expanded at similar rates; however, during stalk elongation (Fig. 2c), WT plants out-competed their ir*AGO7* pairs, attaining significantly longer stalks (Fig. 2c, repeated measures ANOVA, $n = 10$ pairs, $P < 0.01$), greater shoot fresh and dry masses (paired *t*-test, $n = 10$ pairs, $P < 0.01$ for fresh mass and $P < 0.05$ for dry mass), and produced significantly more seed capsules (Fig. 2c, 42%; paired *t*-test, $n = 10$ pairs, $P < 0.01$).

As controls, WT and ir*AGO7* plants were also grown in non-competitive setups (1 plant/pot) under P-limited conditions with AMF, as well as in the above-competitive setup (2 plants/pot) under P-limited conditions but without AMF inoculation. No differences were found between the two genotypes under any of these conditions (Fig. S3).

We evaluated whether the reduced competitive ability of ir*AGO7* is a trait specific for *AGO7*, or if plants silenced in other AGOs (specifically, *AGO1 (a, b, c)*, *AGO2*, *AGO4*, and *AGO10*) were also impaired. Plants were grown in competitive setups under low-P conditions as described earlier and in Fig. 2(c). None of the measured growth and fitness traits differed

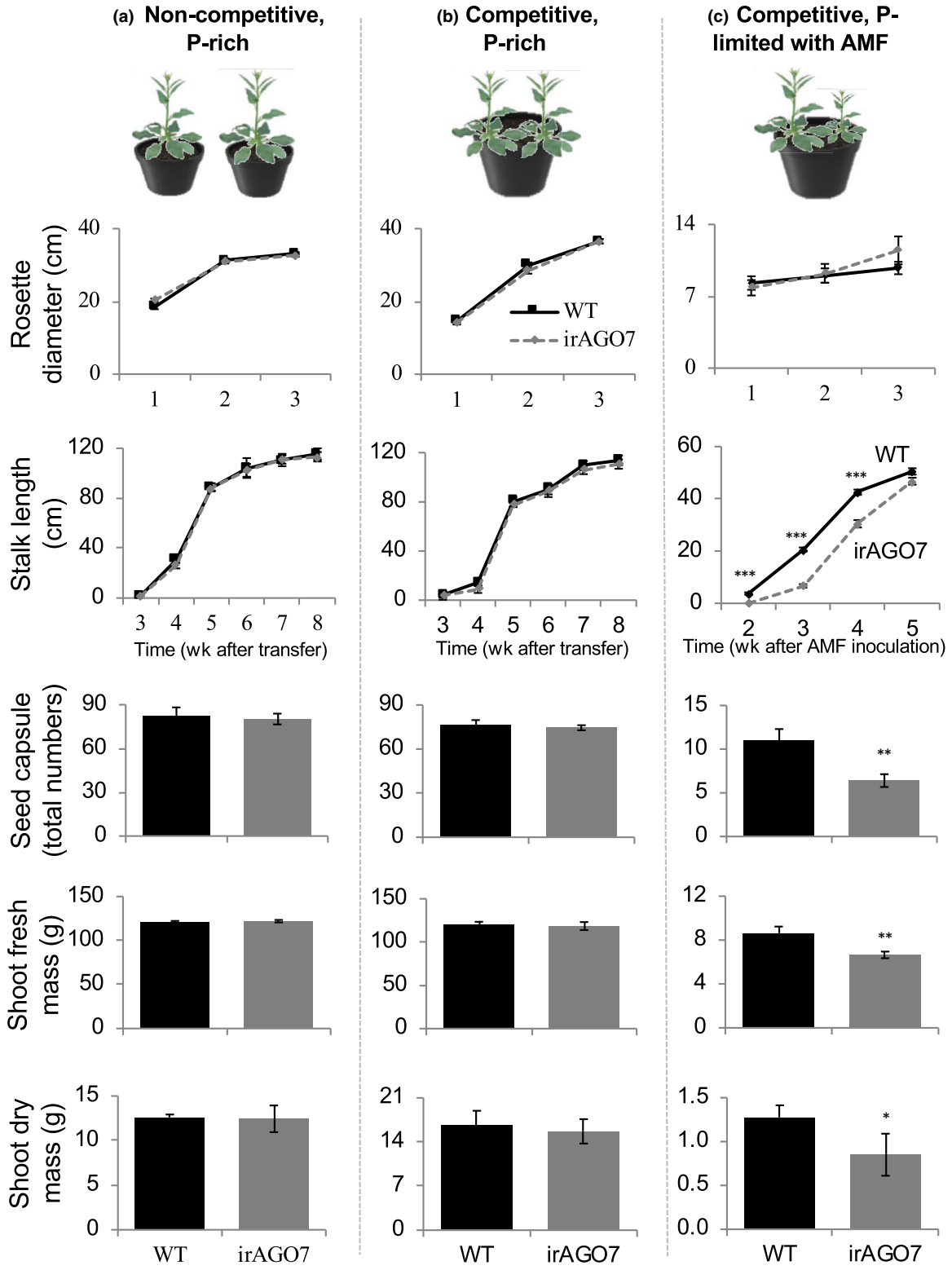

Fig. 2 Silencing *AGO7* impairs *Nicotiana attenuata*'s growth and fitness under P-limited competitive growth with arbuscular mycorrhizal fungi (AMF). (a) Silencing *AGO7* does not affect plant growth and fitness under non-competitive, resource-rich conditions. Rosette diameter, rosette leaf number, chlorophyll content, and total capsule number of ir*AGO7* and wild-type (WT) plants did not differ significantly (values are means ± SD). (b) Similar results were found when plants were grown with WT competitors under P-rich conditions without AMF (values are means ± SD). (c) However, when grown under competitive, P-limited conditions with AMF inoculum, ir*AGO7* plants were out-competed by WT. ir*AGO7* plants had shorter stalk length (*** significantly different from WT, paired *t*-test, $t = 5.387E{-}07$ for 3-wk comparison and $t = 0.00029$ for 4 wk comparison, values are means ± SD, $n = 10$ WT-irAGO7 pairs, $P < 0.001$), significantly lower numbers of seed capsules ($t = 4.048$, $P = 0.013$), as well as less fresh ($t = 4.429$, $P = 0.01$; significant differences designated with **) and dry mass ($t = 3.73$, $P = 0.0187$; significant differences designated with *).

significantly between the WT and the respective ir*AGO* lines (Fig. S4). From these results, we conclude that only ir*AGO7* plants, but not ir*AGO1/2/4/10*, are impaired in their competitive abilities.

AGO7 silencing increases AMF colonization in glasshouse-grown plants

Plants impaired in AMF root colonization (silenced in CCaMK expression) are out-competed by WT or EV competitors (Wang *et al.*, 2018a). Therefore, we evaluated how *AGO7* silencing influenced the AMF-*N. attenuata* interaction (Fig. 3). To access root colonization, we quantified blumenol-C contents as an estimate of arbuscule number (Wang *et al.*, 2018a) of the two genotypes over a period of 8 wk after AMF inoculation (Fig. 3). ir*AGO7* plants had > 2 fold higher blumenol-C levels than those of WT plants at 6 wk after inoculation (Fig. 3a); at 8 wk, the values were still 50% higher in ir*AGO7* (Fig. 3a; repeated measures ANOVA, $n = 10$, $P < 0.01$). None of the other AGOs were altered in their AMF colonization rates as inferred by their leaf blumenol-C contents (Fig. S4). From these results, we infer that silencing *AGO7* increases AMF colonization.

To further evaluate this inference, we estimated root colonization by Trypan Blue staining (Fig. 3b). Total root colonization of ir*AGO7* was > 2 fold greater than that of WT (Fig. 3b; paired *t*-test, $P < 0.01$), which could be clearly seen in the > 2-fold greater number of arbuscules in ir*AGO7* roots (Fig. 3b). Also, mycorrhizal roots and fungal structures were stained by using WGA-fluorescein (WGA-FITC; Fig. S5; Rech *et al.*, 2013) and the data were analyzed according to Trouvelot *et al.* (1986). The results (Fig. 3c) were consistent with the blumenol-C data and Trypan Blue staining in that ir*AGO7* roots were more colonized by AMF as compared to the WT counterparts. Furthermore, at 6 wk post-inoculation, we examined the transcript levels of *RiTEF1α*, a housekeeping gene of *R. irregularis* that is often used as a marker for fungal accumulations (Heck *et al.*, 2016; Voß *et al.*, 2018): *RiTEF1α* transcripts accumulated > 4-fold higher in irAGO7 compared to WT (Fig. 3d), again consistent with enhanced colonization of ir*AGO7* roots by AMF.

Taken together, these results suggest that (only) AGO7 mediates optimal colonization of *N. attenuata* roots by AMF, and silencing of *AGO7* leads to hyper-colonization in glasshouse-grown plants.

AGO7 silencing affects expression of AMF-specific transporters and plant P contents

While ir*AGO7* plants were hyper-colonized by AMF, they still had a reduced competitive ability and we wondered if the arbuscules were fully functional in ir*AGO7* plants. We examined the time-dependent (3, 4 and 6 wk post-AMF inoculation) transcript levels of the AMF-induced host P-transporter, *NaPT4*, in WT and irAGO7 roots. As transcriptional activation of *PT4* is regulated by RAM1 (Pimprikar & Gutjahr, 2018), we also compared transcript levels of *NaRAM1* at the same time points in the two genotypes. In addition, we examined the transcript levels of a *R. irregularis* P-transporter (*RiPT7*) that mediates P-homeostasis of AMF at the symbiotic interface (Xie *et al.*, 2022), and the fungal monosaccharide transporter (*RiMST2*) gene (Xie *et al.*, 2022). In irAGO7 plants, the expression of these genes is deregulated during colonization (Fig. S6). Specifically, P-transporters are strongly down-regulated in ir*AGO7* plants at 6 wk, a time associated with flowering and seed set (Fig. S6).

Next, we evaluated the plant's P-contents. P levels in roots and leaves of ir*AGO7* plants were significantly lower than those in the WT (Fig. 4), which is consistent with the inference that arbuscules might not be fully functional in ir*AGO7* plants.

AGO7 regulates the 'reprogramming' of miRNA accumulation during AMF interactions

As AGOs are the effectors of miRNA-regulatory pathways and impact miRNA accumulations, we next hypothesized that silencing AGO7 might impact AMF-modulated miRNA accumulations. Association of AMF with *N. attenuata* roots dynamically reprograms the accumulation of miRNAs, with several miRNAs accumulating distinct isomiRs depending on AMF colonization status of the roots (Pandey *et al.*, 2018). We selected 35 miRNAs, including six novel miRNAs, from our previous analysis based on their strong differential changes due to AMF and their putative involvement in P-starvation/homeostasis, phytohormone signaling, defense- and stress-response pathways (Pandey *et al.*, 2018). In time-course experiments, we profiled the changes in their abundances in WT and ir*AGO7* roots during early and late stages of colonization.

Complex time/stage- and genotype-dependent changes in miRNA accumulation patterns were evident (Figs 5a, S7, S8). Most (31 of 35) of the miRNAs showed no significant differences in their accumulations between WT and ir*AGO7* roots before AMF inoculation (Fig. S7). After inoculation, 25 were down-regulated in ir*AGO7* roots, mostly during early stages of AMF colonization (up to 3 wk), while the opposite pattern was observed for several miRNAs (e.g. miR160, miR156, miR172, miR482, miR5386) at 6 wk when roots were fully colonized with large numbers of arbuscules of different ages and leaves accumulated high blumenol-C levels (Figs 5a, S8).

Specificity in isomiR-accumulation was also evident (Figs 5a, S8). For example, six sequence variants of miR156 were detected. Most of these miRNAs showed the highest accumulations at 6 wk (Figs 5a, S8). Of these, two (miR156a-5p_2, miR156b-5p) were specifically up-regulated in ir*AGO7* compared to WT only during late root colonization (Figs 5a, S8). Levels of miR172a (both sequence variants) increased after 2 wk of AMF colonization in WT, whereas in ir*AGO7*, their accumulation was significantly enhanced at 6 wk (Figs 5a, S8). miR393a-3p's levels consistently increased in colonized WT, but decreased in ir*AGO7* in early stages; whereas miR393a-5p's accumulation at 6 wk was enhanced in ir*AGO7* (Figs 5a, S8). miR473 was > 2 fold up-regulated in WT at very early stages of AMF root colonization (within 4 d), but in ir*AGO7* plants, again a strong down-regulation was observed (Figs 5a, S8). On the other hand, miR398 was up-regulated in ir*AGO7* specifically during the late

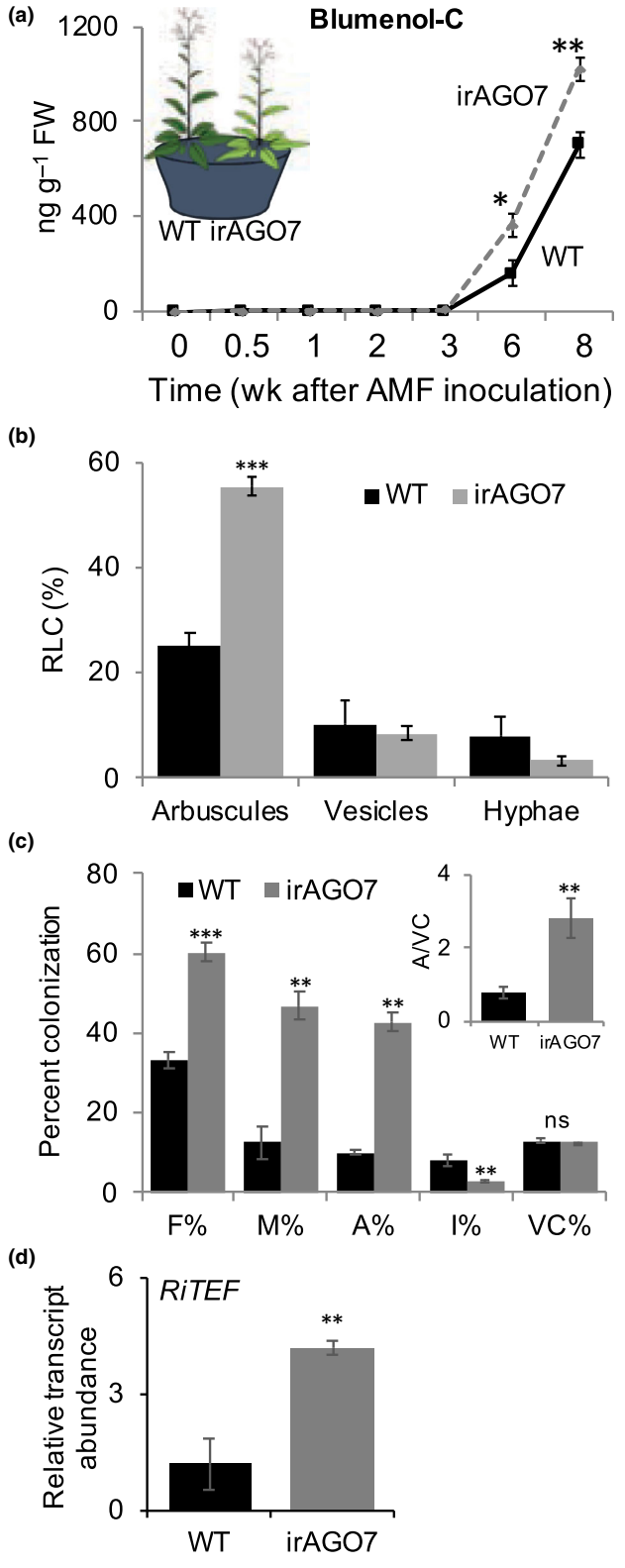

Fig. 3 Silencing *AGO7* increases arbuscular mycorrhizal fungi (AMF) colonization as revealed by leaf blumenol-C levels, microscopic analyses, and gene expression study. (a) When plants are grown under competitive limited-P conditions with AMF (as described in Fig. 2(c)), 6–8 wk after inoculation, the levels of the AMF marker metabolite 11-carboxyblumenol-C glucoside (blumenol-C) were significantly greater in the leaves of *irAGO7* than in those of wild-type (WT) plants. Values are means ± SD (repeated measures ANOVA, $F_{6,30} = 18.50$, $P = 0.007$; * and ** represent significant differences from WT at $P \leq 0.05$ and $P \leq 0.01$; Fishers LSD). (b) Microscopic estimation of AMF colonization structures in WT (black bars) and ir*AGO7* (grey bars) roots, 6-wk post-inoculation, and after staining with Trypan blue. Arbuscules, vesicles, and hyphae were counted. Values presented are means ± SD. *** show significant differences, Wilcoxon signed-rank test, $n = 5$ biological replicates per genotype (50 observations were made on each replicate); $P < 0.001$. (c) AMF colonization structures were also independently investigated with the help of WGA-FITC staining of roots of WT and irAGO7 plants at 6-wk. Quantification of various mycorrhizal structures was carried out using the method of Trouvelot *et al*. (1986). Frequency of colonization in the root system (F%), intensity of colonization (M%), arbuscule abundance (A%), intraradical hyphae abundance (I%), vesicles abundance (VC%), and the ratio of arbuscles to vesicles abundance (A/VC) in the root system were estimated. ***, ** show significant differences between the two genotypes at $P < 0.01$ and $P < 0.05$, respectively (Wilcoxon signed-rank test). (d) Accumulation of *Rhizophagus irregularis Translation Elongation Factor1α* (*RiTEF1α*) transcripts in the roots of AMF colonized WT and irAGO7 plants (6 wk) was analyzed with the help of quantitative real-time PCR assay. *NaECI* gene was used as an internal control; levels in WT were set to 1 and relative expression in irAGO7 was calculated. Error bars show SDs. ** shows significant differences between two genotypes, $n = 3$, $t = 4.03$, $P < 0.01$, paired *t*-test.

stage, whereas miR399's accumulation was more complex, as it was high in WT plants within 2 wk of AMF colonization but this trend reversed at 6 wk, when transcript levels increased in ir*AGO7* plants (Figs 5a, S8). An example of AMF-repressed miRNAs in WT is the novel miRNA, Nat-R-PN59 (Pandey *et al*., 2018), which was consistently down-regulated at all time points in ir*AGO7* (Figs 5a, S8).

Such complex changes in the accumulation of miRNA transcripts during AMF colonization and *AGO7* silencing suggest that *AGO7* functions in their patterns of accumulation.

Silencing AGO7 deregulates gene expression patterns during AMF colonization

The complex changes in miRNA accumulation after AMF inoculation and their dependency on AGO7 motivated us to examine changes in the accumulation of their putative targets. We revisited our previous analysis (Pandey *et al*., 2018) and found 17 genes that corresponded to AMF-related hormone signaling pathways (such as the *SQUAMOSA PROMOTER BINDING PROTEIN-LIKE* (SPL) transcription factors, AP2-type transcription factors, *AFB2*, *GAI1-DELLA*, *EIN3*), P-homeostasis/transport (such as *Laccase 4*, *PHT1-4*) and fatty acid metabolism/transport (such as *PAP12*, *SEC13*, *ALKK*) to be targets of miRNAs 156, 172, 393, 399, 473 and PN59 (Figs 5b–d, S9).

Overall, we observed (1) an inverse pattern of accumulation between ir*AGO7* and WT roots for most of these genes: if a gene was up-regulated after inoculation at a given time-point in WT, it was down-regulated at that time point in ir*AGO7* and vice versa (Figs 5b, S9). (2) Most of the proven/predicted targets show the inverse pattern with their corresponding miRNA levels

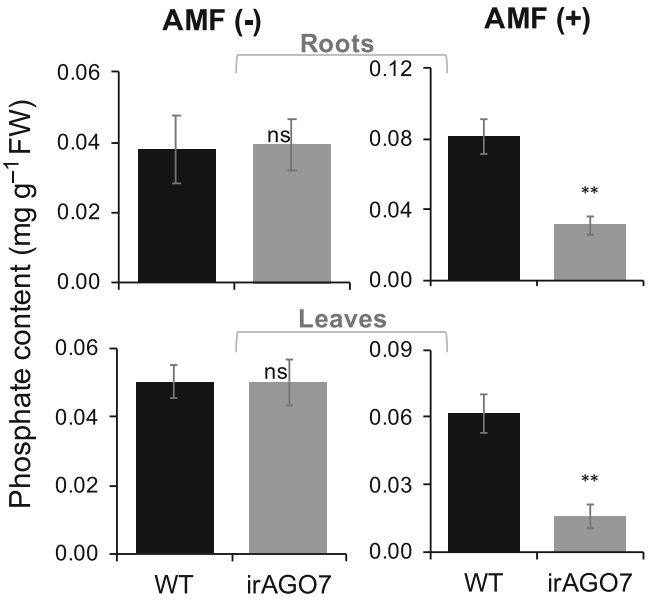

Fig. 4 Silencing AGO7 impairs arbuscular mycorrhizal fungi (AMF)-mediated phosphate accumulation in *Nicotiana attenuata*. Competitively grown wild-type (WT) and irAGO7 pairs of plants were grown for 6 wk in absence (AMF (−); left panel) and presence (AMF (+); right panel) of *Rhizophagus irregularis*, similar to those described in Figs 2(c) and 3. Roots (upper panel) and leaves (lower panel) of these plants were assayed for their phosphate contents; all the values are means ± SD. ** indicates significant differences in between WT and irAGO7 genotypes, paired *t*-test; $n = 6$, $t_{root} = 4.54$, $P_{root} < 0.01$; $t_{leaves} = 4.29$, $P_{leaves} < 0.01$; ns indicates no significant differences between phosphate levels between the tissues of the two genotypes.

(Fig. 5c). (3) The commonly observed 'one-many:: many-one' relationship of targets and miRNAs was apparent, and these could be distinguished as being operational at early and late stages of AMF colonization (Fig. 5c). For example, miR156 is known to target the SPLs that respond to auxin signaling (Sunkar *et al.*, 2012; Yu *et al.*, 2015; Xu *et al.*, 2016). Interestingly, the miR156-*SPL3* module regulates phosphate-deficiency response (Lei *et al.*, 2015; Xu *et al.*, 2016), whereas the miR156-*SPL9* module also regulates reactive oxygen species accumulation (Yin *et al.*, 2019). While the binding of SPL with other regulators, such as DELLAs, interfere with their activity/expression (Zhang *et al.*, 2019), SPLs also positively regulate the accumulation of miRNAs in a negative feedback loop (Yu *et al.*, 2015). A strong up-regulation of *SPL3* was noticed in ir*AGO7* during the early stages of colonization (3 wk), whereas *SPL9* transcripts accumulated significantly more at 6 wk in WT plants (Figs 5b, S9). Furthermore, *AFB2*- an auxin signaling component (and miR393-proven target) was strongly up-regulated at 3 wk in ir*AGO7* (Figs 5b, S9).

miR172 acts sequentially with miR156, is positively regulated by SPL9 (Wu *et al.*, 2009), and targets a number of genes such as *RAP2-7*, *AP2*, *APL*, and *PEX14*. All of these genes were strongly up-regulated in WT plants at 6 wk, and the transcript levels of these genes were low in ir*AGO7* plants (Figs 5b, S9). *PUB45*, putative target of miR393 and Nat-R-PN59, was weakly expressed in ir*AGO7* plants during the early stages of colonization, while it was up-regulated in ir*AGO7* at late stages compared to WT (Figs 5b, S9).

The transcript levels of *DELLA-GAI1* and *PAP12* (putative targets of miR473), *EIN3* (putative target of miR-PN59), and the miR399-related genes *PHT1-4* and *IRX12 laccase4* were low in ir*AGO7* across all time points after AMF root colonization. miR399, along with PHO2, is reported to regulate the expression of PHT1-4 phosphate transporter during salt stress response of Arabidopsis (Pegler *et al.*, 2020).

From the earlier mentioned data, we infer that miR156, 172, 393, 399, 473 and the novel miRNA-PN59 participate in regulating hormone signaling, P-related pathways, vegetative-adult phase transition, fatty acid metabolism, and oxidative stress response (Fig. 5d). Although many of these pathways are implicated in host–AMF interaction, the biological functions of these miRNAs in the context of plant fitness during colonization by AMF remain poorly explored.

AGO7-influenced miRNAs regulate AMF colonization and plant fitness

To test the inference that the earlier mentioned miRNAs are functionally relevant in host–AMF interactions and plant fitness, we overexpressed five conserved miRNAs (miR156b-5p (ov156), miR172-3p_1 (ov172), miR399a-3p_3 (ov399), miR393a-5p (ov393), miR473-5p_2 (ov473) and the novel miR-Nat-R-PN59 (ovPN59)) in WT *N. attenuata* plants (Figs 6, S10; Table S3). In addition, we tested the role of Na-miR398 (ov398) in plant–AMF interactions as this miRNA was implicated in nutrient homeostasis and oxidative stress/abiotic stress responses (Zhu *et al.*, 2011). Na-miR398 is strongly differentially regulated during *Nicotiana*–AMF interactions, but whether miR398 has a direct influence on AMF colonization is unknown.

We evaluated how overexpression of these miRNAs affected AMF colonization, plant growth, and reproductive performance (Figs 6, S11). miR156 overexpression strongly reduced stalk length and capsule production, whereas it significantly increased AMF colonization by *c.* 50% (Fig. 6). By contrast, overexpression of a Na-miR172 only marginally reduced stalk lengths but strongly influenced seed capsule production (Fig. 6); however, AMF colonization was not significantly affected. miR399 overexpression although did not influence stalk length, it reduced capsule production and AMF colonization (Fig. 6). By contrast, overexpression of miR393 did not influence plant height or overall capsule production (although a delay was recorded), whereas it increased AMF colonization (Fig. 6). Interestingly, ov398 plants strongly reduced AMF colonization, and were initially smaller than the EV, and produced fewer capsules 5–6 wk after inoculation, but at the 8-wk time point, they produced the same number of capsules as the EV plants (Fig. 6). Overexpression of miR473 and Na-R-PN59 (ov473 and ovPN59) reduced AMF colonization and strongly reduced plant fitness: ov473 as well as ovPN59 plants showed no difference in rosette to elongation transition, whereas both genotypes were shorter and produced fewer capsules (Fig. 6). In summary, overexpression of miR156

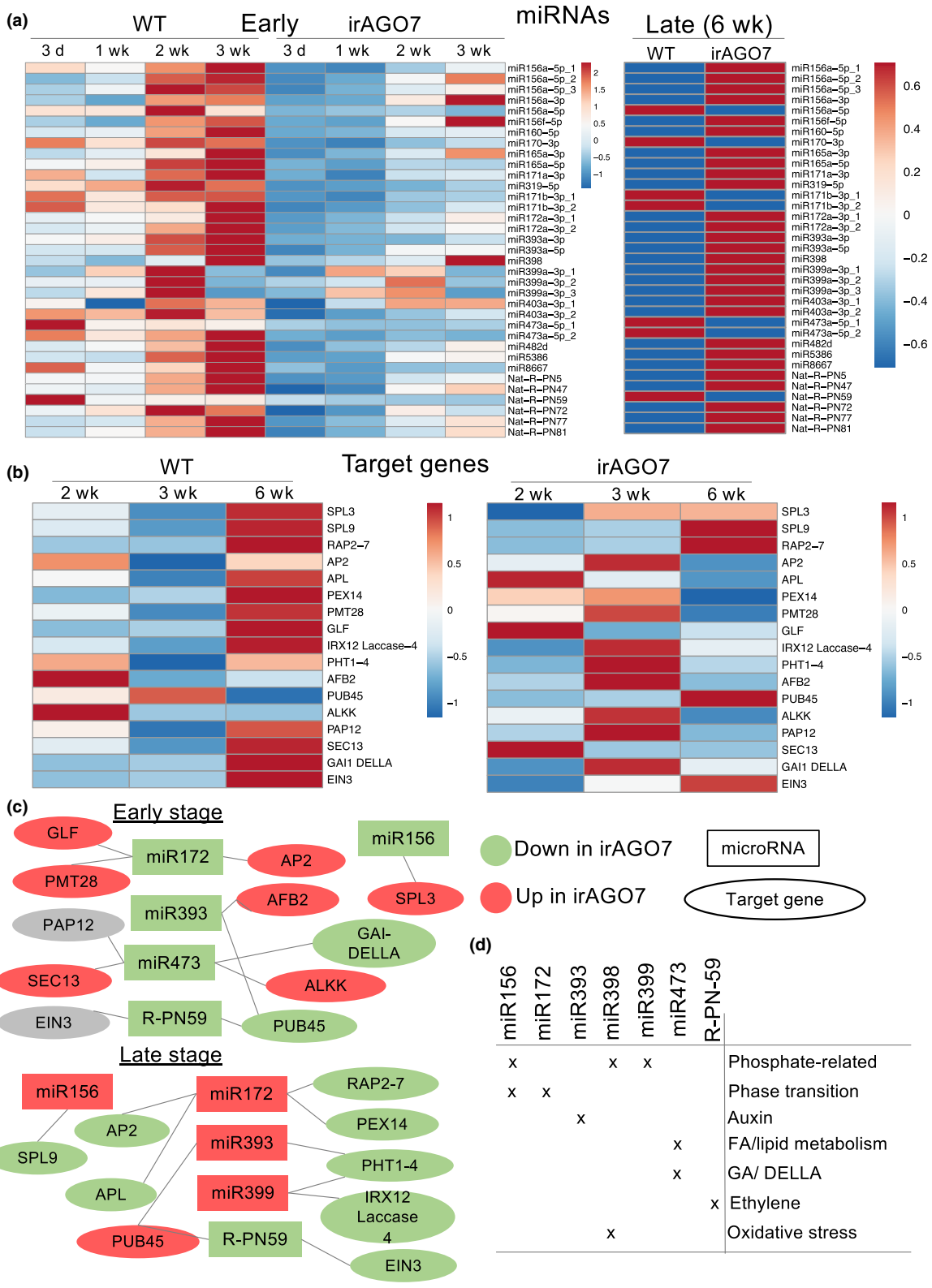

and miR393 promoted AMF colonization, whereas miR398, miR399, miR473, and Na-R-PN59 reduced colonization, while the sequence of miR172 used in overexpression appeared not to be decisive for this symbiosis (Fig. 6).

To gain further insights, we investigated how the transcript levels of target genes were altered by overexpression of miR473 and the novel Na-R-PN59 miRNA. miR473 targets three genes of the fatty acid/lipid metabolism pathway (*ALKK*, *PAP12*, and

Fig. 5 Temporal dynamics of arbuscular mycorrhizal fungi (AMF)-influenced miRNAs and their putative targets in wild-type (WT) and AGO7-silenced (ir*AGO7*) plants during the process of AMF colonization. Relative abundances during AMF colonization compared to uninoculated control (time 0) were calculated (detailed in Supporting Information Figs S8, S9) and heat maps were generated with the help of ClustVis server (https://biit.cs.ut.ee/clustvis/) after rows were centered and unit variance scaling was applied to rows. (a) Change in accumulation patterns of 35 miRNAs ($n = 3$–4; further detailed in Fig. S8) in WT and ir*AGO7* roots during early stages of AMF colonization (3 d to 3 wk; left panel) and at 6 wk after colonization was determined. (b) Changes in accumulation of transcripts of 17 miRNA target genes participating in phosphate-related processes, hormone signaling, phase transition, and fatty acid metabolism were determined during the process of AMF colonization (2–3 wk) and after 6 wk in WT and ir*AGO7* roots ($n = 3$–4; further detailed in Fig. S9). microRNA–target relationships and directionality of their accumulation in ir*AGO7* are presented in (c). For most of the miRNA–target pairs, an inverse relationship was noticed. Panel (d) represents the biological processes/pathways that might be modulated (shown with 'x') by seven miRNAs, whose functional role in plant–AMF interaction is further tested in our study.

SEC13), and a *GAI-DELLA* (GA signaling). *ALKK* and *PAB12* transcripts were very strongly reduced, and *GAI-DELLA*'s transcript was also abolished in ov473 plants as compared to EV controls (Fig. 7). miR-Nat-R-PN59 targets ET signaling pathways by targeting *EIN3* and *PUB45*: levels of both genes was strongly attenuated by overexpression of this miRNA (Fig. 7). Furthermore, we tested whether reproductive performance (stalk length and seed capsule production) was altered when plants overexpressing miR473 or PN59 were grown in the absence of AMF: no differences were observed (Fig. S12). These findings suggest that these miRNAs play a role in modulating reproductive performance and AMF root colonization probably by regulating fatty acid metabolism, GA signaling, and ET signaling pathways.

Discussion

Here, we examined the biological function of *N. attenuata*'s *AGO7*. We infer that *NaAGO7* does not directly regulate developmental traits. However, when grown in competition under low-P conditions with AMF in the glasshouse, or under field conditions, ir*AGO7* plants had severely reduced competitive reproductive output (Figs 1, 2), while losses to pathogens and herbivores were similar to those of WT plants. Reduced fitness under competitive P-limited growth conditions was specific for ir*AGO7*; silencing other *NaAGO*s did not decrease plant performance under these conditions (Fig. S4). Here, we propose that *AGO7* affects the plant's competitive capacity under P-limited conditions due to hyper-colonization by AMF. When colonized by AMF, plants recruit an AGO7-related smRNA pathway that modulates gene-expression networks of various signaling components so that symbiotic outcomes are optimized (Fig. 8). In the following sections, we evaluate the literature regarding our inferences on the whole-plant consequences of AGO7 silencing and follow these with evaluations of AGO7's role in symbiotic signaling.

The function of several AGOs, in particular AGO7, remains unknown or is only described for a few species. An Arabidopsis *AGO7* mutant (*ZIPPY*) was first characterized by its premature change in leaf morphology (Hunter *et al.*, 2003). Similarly, in maize and rice, *AGO7* mutations affected leaf development (Nagasaki *et al.*, 2007; Douglas *et al.*, 2010). However, in *N. attenuata*, we were surprised not to find similar phenotypes in -AGO7-silenced plants. Two hypotheses could account for this discrepancy. In ir*AGO7* lines, residual amounts of AGO7 activity might be sufficient to execute these developmental processes. Alternatively, AGO7 may have acquired a novel function in *N. attenuata* as a consequence of the unique selection pressures that this species encounters (Navarro-Quezada *et al.*, 2020). AGOs' sequences, structures, and functions are constantly evolving, likely a result of changing selection pressures (Singh *et al.*, 2015; Singh & Pandey, 2015; Pradhan *et al.*, 2017, 2021). Studies on AGO7 function in legume–rhizobia interactions provide hints that similar regulatory processes may operate between these two types of symbiotic interactions.

Mutations in *Medicago truncatula AGO7* enhanced nodulation and rhizobial infection (Hobecker *et al.*, 2017), a pattern which was similar to our findings for AMF interactions. Legumes auto-regulate nodulation to avoid hyper-nodulation (Penmetsa *et al.*, 2003; Schnabel *et al.*, 2005). Na*AGO7* may play a similar role in the plant–AMF symbiosis – regulating the number of arbuscules to temper symbiotic costs. Host plants provide photo-assimilates in quantities that approach 20% of net primary productivity to the fungus in exchange for P and other micronutrients (Smith & Smith, 2011). Hyper-colonization may increase these already high investment costs. The large number of arbuscules in ir*AGO7* plants may not be fully functional, potentially leading to a feedback loop that increases arbuscule production further.

The auto-regulation of arbuscules is likely initiated early during the host-AMF interaction, where the negative self-regulation of colonization occurs independently of a plant's P-status (Müller *et al.*, 2019). Results from studies that manipulated CLE (CLAVATE3/EST-related) peptide or CLAVATA (CLV) expressions (Müller *et al.*, 2019) are consistent with the inference that over-colonization by AMF does not always increase host fitness. Rather, enhanced AMF colonization has severe consequences for growth and reproduction (Morandi *et al.*, 2000; Solaiman *et al.*, 2000; C. Wang *et al.*, 2018; Müller *et al.*, 2019). These studies are consistent with the observations that hypercolonization of ir*AGO7* negatively affects fitness in *N. attenuata*. The overarching scenario is consistent with the observations of reduced phosphate levels (Fig. 4), and suppressed transporter gene expression in reproductive-stage plants (Fig. S6), collectively suggesting that lower resource mobilization in ir*AGO7* plants could explain their reduced reproductive output.

The effects of *AGO7* silencing on AMF-related signaling appears to be far-reaching. During AMF colonization, *N. attenuata* changes its miRNA profile (Pandey *et al.*, 2018). Kinetic analyses of AMF-changed miRNAs and their putative targets in ir*AGO7* and WT roots clearly revealed the expected negative relationships (Fig. 5), consistent with the inference that the miRNAs may relate to their target genes with AGO7 as a central regulator. In the following sections, we discuss the role of

these miRNAs in plant–AMF interaction in the context of nutrient investment, root colonization, and phytohormone signaling.

In the context of nutrient investment, the accumulation patterns of miR398 and the three miR399-sequence variants are interesting. These miRNAs are likely involved in regulating P-starvation responses and nutrient deficiencies (Hsieh *et al.*, 2009; Kuo & Chiou, 2011). The accumulation pattern of miR399 inversely corresponds with that of its putative targets, *laccase 4* and phosphate transporter *PHT1-4*, at 6 wk. A down-regulation of *PHT1* was also observed in Arabidopsis plants

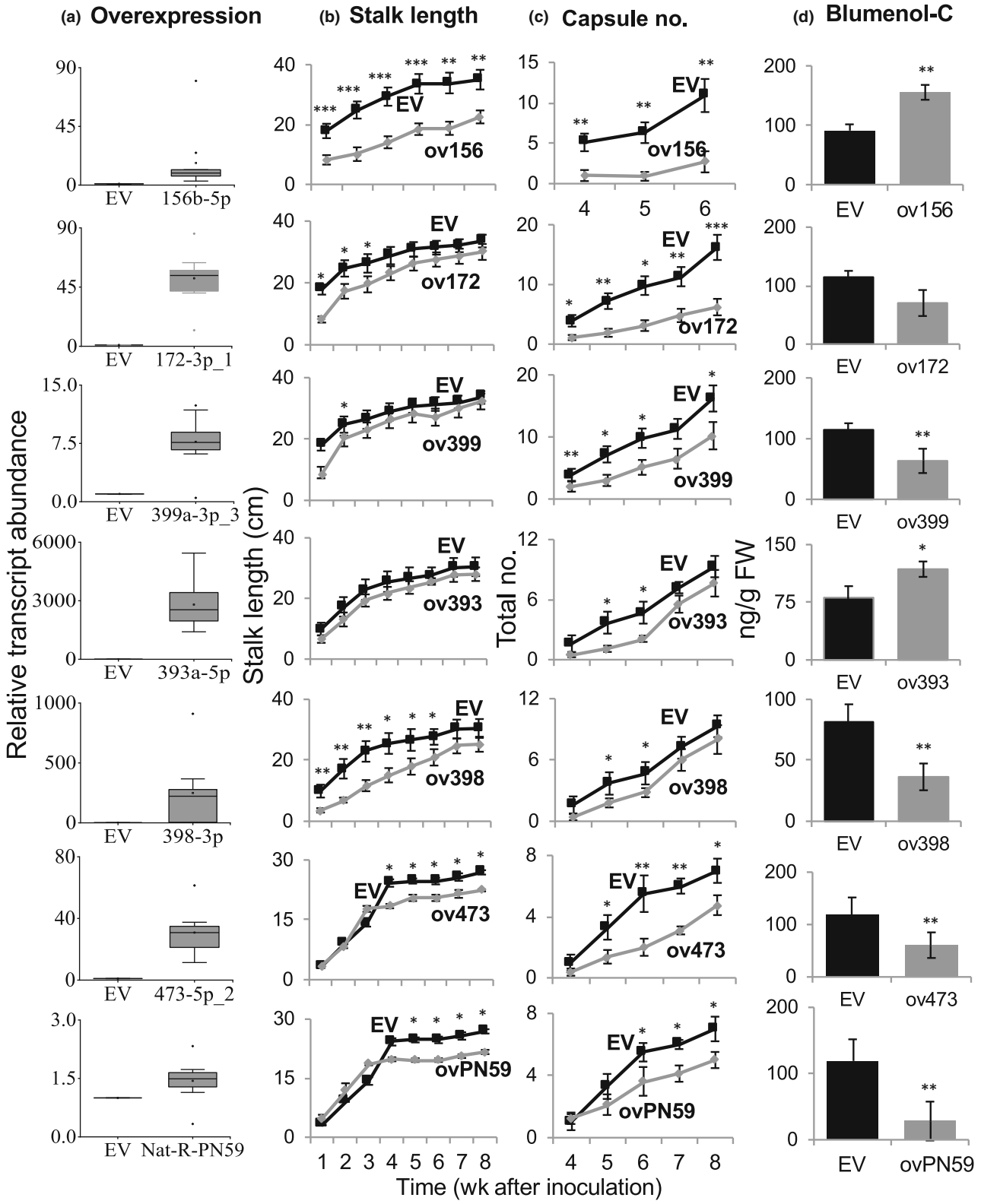

Fig. 6 Evaluation of miRNA functions during host–arbuscular mycorrhizal fungi (AMF) interaction. Seven miRNAs were transiently overexpressed to evaluate their influence on plant fitness and host–AMF interactions under low-P conditions. miRNAs were transiently overexpressed (ov) in wild-type (WT) *Nicotiana attenuata* plants (vectors described in Supporting Information Fig. S10). (a) Overexpression was quantified with the help of miRNA-qPCR assays. Level of a miRNA in empty vector (EV)-inoculated WT plants was set to 1 and relative fold increase in miRNA abundance in plants overexpressing a particular miRNA construct was determined. Effect of miRNA-overexpression on plant fitness was determined by comparing increases in stalk length (b) and seed capsule production (c), while effects on AMF colonization rates was determined by measuring blumenol-C contents in leaves at 6 wk (d). The plants were grown individually in 1 l pots. Significant differences were measured with the help of two-way repeated measures ANOVA for (b, c) and one way ANOVA for (a, d), values presented are means ± SD, number of biological replicates (n) = 8–12. *, **, and *** show significant differences for a trait between WT and ir*AGO7* at a given time point at $P < 0.05$, $P < 0.01$, and $P < 0.005$, respectively. Additional details on test statistics are provided in Table S3.

overexpressing miR399 (Fujii *et al.*, 2005). In Arabidopsis, miR398 is down-regulated under P-starvation, while in tomato it is increased (Pant *et al.*, 2009; Gu *et al.*, 2010; Zhu *et al.*, 2011). Also, miR398 may be involved in alleviating oxidative stress (Sunkar *et al.*, 2006; Zhu *et al.*, 2011). Significant reductions in AMF colonization and growth were observed upon the overexpression of miR399 and miR398 (Fig. 6).

The role of miR399 in plant–AMF interactions appears to be complex. In *M. truncatula*, miR399 levels are increased in AMF-colonized roots under P-limited conditions (Branscheid *et al.*, 2010). This is similar to our results for ir*AGO7* and consistent with the hypothesis that miR399 is locally induced to maintain continuous root colonization (Branscheid *et al.*, 2010). However, overexpression of an Arabidopsis miR399-homolog (ath-miR399d) in tobacco did not influence mycorrhizal colonization (Branscheid *et al.*, 2010). But plants have several miR399 sequence variants (e.g. 15 in *M. truncatula*; Branscheid *et al.*, 2010) and their interplay in AMF-symbiosis is unknown. In *N. attenuata*, we had previously found a strong upregulation of miR399 in AMF-colonized roots in plants impaired in AMF colonization growing in competition with a fully functional partner, while these plants had a lower total P content (Pandey *et al.*, 2018; Wang *et al.*, 2018a). These results are consistent with those obtained here when miR399 in *N. attenuata* was overexpressed, leading to lower AMF colonization rates compared to WT. It is well known that nutrient starvation responses are a complex interplay of local and systemic responses, in which particular systemic leaf signals are important for nutrient acquisition (Carbonnel & Gutjahr, 2014; Chien *et al.*, 2018). Moreover, phytohormone signaling is yet another layer of regulators of AMF symbiosis and AGO7-modulated miRNAs could be a central player in these phytohormone-mediated responses.

Plant–AMF interactions result in a complex modulation of GA, ET, and auxin signaling, which interact synergistically as well as antagonistically (Gutjahr, 2014; Fracetto *et al.*, 2017; Liao *et al.*, 2018). We propose that this hormonal crosstalk is mediated by miRNAs in an AGO7-dependent manner. For instance, GA plays a complex role during various stages in the symbiosis (Tominaga *et al.*, 2019). GA inhibits, as well as promotes, the infection and colonization of AMF in a host (Takeda *et al.*, 2015). GA influences several aspects of hyphal entry and branching through its influence on the expression of several critical genes and transcription factors, including RAM1 and SbtM1 (Takeda *et al.*, 2015). GA levels are finely regulated in roots for optimal colonization (Martín-Rodríguez *et al.*, 2015). Low GA suppresses colonization, whereas high GA levels can inhibit AMF entry (Takeda *et al.*, 2015). DELLA proteins act as coordinators of GA action during endosymbiosis (Fonouni-Farde *et al.*, 2016). Our results suggest that miRNAs play a central role in regulating the GA pathway. For instance, NamiR473-mediated DELLA-assisted regulation of GA could fine-tune its action and facilitate optimal colonization.

The overexpression of Na-miR473 and Na-R-PN59 resulted in reduced AMF colonization. miR473 targets genes related to GA signaling and fatty acid metabolism. DELLAs are required for arbuscule formation and nutrient transfer (Floss *et al.*, 2013; Foo *et al.*, 2013; Yu *et al.*, 2014; Park *et al.*, 2015), as sugars and fatty acids are traded between plants and fungi (Keymer *et al.*, 2017; Luginbuehl *et al.*, 2017). It is plausible that overexpression of miR473 reduced colonization by significantly reducing *ALKK*, *PAP12*, and *GAI1-DELLA* transcript levels. Similarly, overexpression of Na-R-PN59 strongly attenuated the transcript levels of *PUB45* and *EIN3* (ET signaling) targets, while AMF colonization rates were significantly lower. The biological functions of these two miRNAs were not previously known in plant–AMF interaction, but EIN3 acts down-stream of EIN2 in ET signaling (Dolgikh *et al.*, 2019).

ET acts as a negative regulator of AMF entry and root colonization and balances the beneficial and non-beneficial traits of this endophytic interaction (Camehl *et al.*, 2010; Mukherjee & Ané, 2011). ET negatively regulates the Sym and non-Sym pathways (Mukherjee & Ané, 2011), negatively modulates the repressing effect of Pi on AMF symbiosis and regulates a host's Pi-starvation response pathway (Torres de los Santos *et al.*, 2016). ET interacts with other hormones (like GA) during symbiosis in complex ways (Martín-Rodríguez *et al.*, 2011; Foo *et al.*, 2016). Unregulated ET production in a host may falsely signal deficiencies of other hormones, such as ABA, with detrimental effects for the symbiosis (Fracetto *et al.*, 2017). Therefore, ET levels need to be fine-tuned for successful symbiosis, and AGO7-related miRNAs, such as Na-miR473 and Na-R-PN59, may provide the required regulatory network. Overall, the role of ET signaling in the AMF symbiosis still has several unsolved aspects (Foo *et al.*, 2013), and our results add a piece to this puzzle – here, abrogation of the ET signaling pathway clearly correlates with significantly reduced AMF colonization. Further studies including ET measurements are required to better understand how ET affects the AMF symbiosis. As GA and ET signaling pathways interact (Foo *et al.*, 2016), perhaps these miRNAs mediate their cross-talk during arbuscule formation.

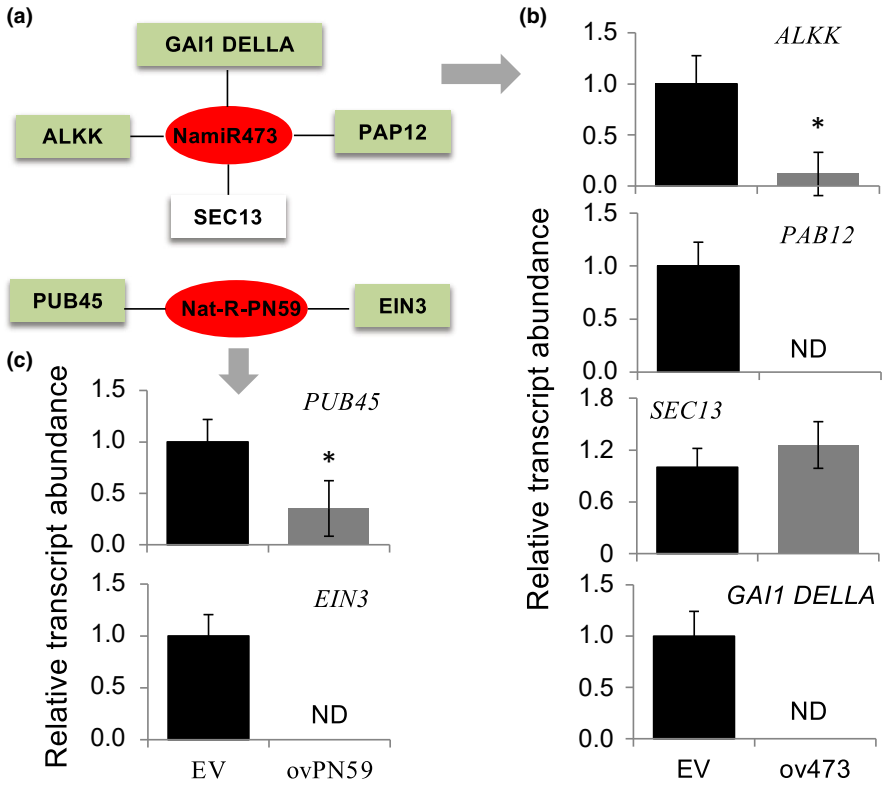

Fig. 7 Overexpression of miR473 and miR Na-R-PN59 down-regulates their targets in gibberellic acid (GA), fatty acid metabolism and ethylene pathways during plant–arbuscular mycorrhizal fungi (AMF) interaction. (a) Depicts four predicted targets of miR473 and the two targets of the novel Nat-R-PN59 miRNA, respectively. (b) Increased abundance of miR473 (red oval, a) strongly down-regulates 3 of 4 target genes (green rectangles, a). Similarly, (c) overexpression of the novel Nat-R-PN59 down-regulates both of its targets. Target accumulation was evaluated by qPCR assays. Levels in empty vector (EV) plants were set to 1 and relative expression in plants overexpression (ov) a miRNA were calculated. ND transcript not detectable; one-way ANOVA, Fisher's LSD, for *PUB45*, $F = 2.09$, $P = 0.052$ and for *ALKK*, $F = 15.79$, $P = 0.007$, values presented are means ± SD, number of biological replicates (n) = 4. * significantly different from EV, $P < 0.05$.

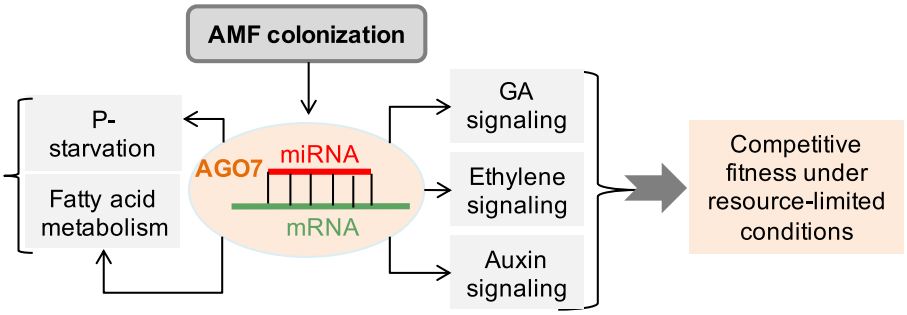

Fig. 8 A model showing the role of AGO7 in modulating several aspects of host–arbuscular mycorrhizal fungi (AMF) interaction.

During early time points of root colonization (3 d to 3 wk after inoculation), when AMF starts to enter the plants and form the first arbuscules (Pimprikar & Gutjahr, 2018), miRNAs were mostly up-regulated in AMF-colonized WT roots compared with ir*AGO7*. However, at later stages, when arbuscules mature, the miRNA levels were reversed (or equalized). This pattern is well represented by miR393a. miR393 regulates *TIR* and several *AFB* genes, encoding auxin receptors (Navarro *et al.*, 2006; Vidal *et al.*, 2010), and in concert with miR390, regulates lateral root development (Lu *et al.*, 2018). The miR390/TAS3 module plays a role in nodulation of *M. truncatula* (Hobecker *et al.*, 2017). Earlier, we found that AMF colonization increased miR390 accumulation in *N. attenuata* (Pandey *et al.*, 2018), but subsequent research into miR390-function in this species by stable overexpression did not find a role in AMF symbiosis; instead miR390 modulates plant tolerance responses to herbivory (Pradhan *et al.*, 2021).

miR393 is considered a negative regulator of arbuscule formation because its overexpression in three plant species strongly impairs arbuscule formation (Etemadi *et al.*, 2014). While this appears to contradict our findings, comparisons of AMF-inoculated with non-inoculated *N. attenuata* plants clearly showed a down-regulation of miR393a-3p (Pandey *et al.*, 2018). Here too, we see a negative correlation between transcript levels of miR393a-5p with its *AFB2* target. During early stages of colonization (2–3 wk), miR393 levels are low in ir*AGO7* plants (compared to WT), while *AFB2* levels are high (Fig. 5c), which might promote colonization (as seen in irAGO7). *AFB2*'s decrease at 6 wk might be associated with a putative auto-regulatory feedback loop controlling arbuscule numbers. Increased miR393 levels in ir*AGO7* at 6 wk, corresponding with decreased *AFB2* levels, along with ir*AGO7*'s increased colonization and reduced fitness are consistent with the gain-of-function analyses as plants overexpressing this miRNA have increased

colonization but marginally reduced fitness. Moreover, auxin signaling and its response factors also engage with other miRNAs, such as miR172 and miR156.

The two sequence variants of miR172a showed accumulation patterns similar to that of miR393a. miR172a plays a role in the rhizobium–lotus interaction and strongly accumulates with nodulation (Nod) factor and compatible rhizobia (Holt *et al.*, 2015). Overexpression of miR172 in *N. attenuata* interestingly did not significantly affect AMF colonization but severely impaired plant fitness. Taken together, results of overexpression of miR393 and miR172 analyses indicates synergistic actions of these two miRNAs, and plausibly a conserved function, as in other species, in regulating auxin signaling.

The accumulation pattern of miR156a sequence variants was even more complex and strongly variable. In *Lotus japonicus*, ectopic expression of miR156a led to enhanced branching, delayed flowering, underdeveloped roots, reduced nodulation, and repression of several nodulation genes (Wang & Chua, 2014). Its function in AMF had not been described, although it was speculated that it might act similarly to miR171b, having a positive effect on symbiosis (Couzigou *et al.*, 2017). Indeed, in ir*AGO7*, most isomiRs were highly up-regulated at 6 wk post-inoculation when significantly higher AMF colonization rates were also observed. Overexpression of the miR156b-5p variant suggests that miR156 might have a positive effect on the AMF symbiosis, but its overexpression might negatively impact a plant's reproductive performance. Moreover, we found a higher transcript abundance of miR171b during early stages of root colonization in AMF-colonized WT than in ir*AGO7* roots; during the mature stage of AMF colonization, miR171a, which acts as a repressor of AMF colonization in *L. japonicus* (Couzigou *et al.*, 2017), is enriched in ir*AGO7* compared with WT plants. Further studies are needed to resolve this complexity.

In conclusion, we infer that a complex network of miRNAs is deployed during plant–AMF interactions, which is modulated by AGO7. AGO7 participates in the AMF-induced smRNA pathway to control root colonization through the actions of various phytohormone signaling and phosphate starvation/transport responses (Fig. 8). Knockdown of AGO7 destabilizes/disrupts regulatory networks and reverses the outcomes of several miRNA–mRNA interactions. The mechanistic basis of recruitment of miRNAs by AGO7 during host–AMF interaction needs further study as AGO7 might be involved in the differential accumulation and recruitment of AMF-associated miRNAs and multiple checkpoints and sequence-dependent recruitment mechanisms cannot be ruled out.

Acknowledgements

We thank the glasshouse team of the Max Planck Institute for Chemical Ecology for plant cultivation and the Brigham Young University for use of their field station, the Lytle Ranch Preserve. We also thank Dr Karin Groten for help with the initial experiments as well as constructive discussions, and Dr Klaus Gase for making the overexpression constructs. Help from Adithi Vasudevan in processing of roots samples is thankfully acknowledged. Ling Chuang's help with the field work is also thankfully acknowledged. This work was supported by the Max Planck Society's core funding of ITB's Department, and the Deutsche Forschungsgemeinschaft (DFG, German Research Foundation) – SFB 1127/2 ChemBioSys – 239748522 to ITB. Open Access funding enabled and organized by Projekt DEAL.

Competing interests

None declared.

Author contributions

SPP and ITB conceived the original research plan; MP, ITB, and SPP designed the research; MP and SPP carried out experiments; SPP, MP and ITB carried out field work; SPP, MP and ITB wrote the manuscript; ITB provided most of the resources.

ORCID

Ian T. Baldwin https://orcid.org/0000-0001-5371-2974
Shree P. Pandey https://orcid.org/0000-0002-4546-9123
Maitree Pradhan https://orcid.org/0000-0002-9279-640X

Data availability

The data that support the findings of this study are available in the Supporting Information of this article.

References

Axtell MJ. 2013. Classification and comparison of small RNAs from plants. *Annual Review of Plant Biology* **64**: 137–159.

Baldwin IT, Morse L. 1994. Up in smoke 2. Germination of *Nicotiana attenuata* in response to smoke-derived cues and nutrients in burned and unburned soils. *Journal of Chemical Ecology* **20**: 2373–2391.

Borges F, Martienssen RA. 2015. The expanding world of small RNAs in plants. *Nature Reviews. Molecular Cell Biology* **16**: 727–741.

Bozorov TA, Baldwin IT, Kim S-G. 2012a. Identification and profiling of miRNAs during herbivory reveals jasmonate-dependent and -independent patterns of accumulation in *Nicotiana attenuata*. *BMC Plant Biology* **12**: 209.

Bozorov TA, Pandey SP, Dinh ST, Kim SG, Heinrich M, Gase K, Baldwin IT. 2012b. DICER-like proteins and their role in plant-herbivore interactions in *Nicotiana attenuata*. *Journal of Integrative Plant Biology* **54**: 189–206.

Branscheid A, Sieh D, Pant BD, May P, Devers EA, Elkrog A, Schauser L, Scheible W-R, Krajinski F. 2010. Expression pattern suggests a role of miR399 in the regulation of the cellular response to local Pi increase during arbuscular mycorrhizal symbiosis. *Molecular Plant–Microbe Interactions* **23**: 915–926.

Brant EJ, Budak H. 2018. Plant small non-coding RNAs and rheir roles in biotic stresses. *Frontiers in Plant Science* **9**: 1038.

Brundrett MC, Piché Y, Peterson RL. 1984. A new method for observing the morphology of vesicular–arbuscular mycorrhizae. *Canadian Journal of Botany* **62**: 2128–2134.

Bubner B, Baldwin IT. 2004. Use of real-time PCR for determining copy number and zygosity in transgenic plants. *Plant Cell Reports* **23**: 263–271.

Bubner B, Gase K, Baldwin IT. 2004. Two-fold differences are the detection limit for determining transgene copy numbers in plants by real-time PCR. *BMC Biotechnology* **4**: 1–14.

Camehl I, Sherameti I, Venus Y, Bethke G, Varma A, Lee J, Oelmüller R. 2010. Ethylene signalling and ethylene-targeted transcription factors are required to balance beneficial and nonbeneficial traits in the symbiosis between the endophytic fungus *Piriformospora indica* and *Arabidopsis thaliana*. *New Phytologist* **185**: 1062–1073.

Carbonell A. 2017. Plant ARGONAUTEs: features, functions, and unknowns. In: Carbonell A, ed. *Plant Argonaute proteins: methods and protocols*. New York, NY, USA: Springer, 1–21.

Carbonnel S, Gutjahr C. 2014. Control of arbuscular mycorrhiza development by nutrient signals. *Frontiers in Plant Science* **5**: 462.

Chien P-S, Chiang C-P, Leong SJ, Chiou T-J. 2018. Sensing and signaling of phosphate starvation: from local to long distance. *Plant and Cell Physiology* **59**: 1714–1722.

Choi J, Summers W, Paszkowski U. 2018. Mechanisms underlying establishment of arbuscular mycorrhizal symbioses. *Annual Review of Phytopathology* **56**: 135–160.

Couzigou JM, Combier JP. 2016. Plant microRNAs: key regulators of root architecture and biotic interactions. *New Phytologist* **212**: 22–35.

Couzigou J-M, Lauressergues D, André O, Gutjahr C, Guillotin B, Bécard G, Combier J-P. 2017. Positive gene regulation by a natural protective miRNA enables arbuscular mycorrhizal symbiosis. *Cell Host & Microbe* **21**: 106–112.

Cuperus JT, Montgomery TA, Fahlgren N, Burke RT, Townsend T, Sullivan CM, Carrington JC. 2009. Identification of MIR390a precursor processing-defective mutants in Arabidopsis by direct genome sequencing. *Proceedings of the National Academy of Sciences, USA* **107**: 466–471.

Dolgikh VA, Pukhovaya EM, Zemlyanskaya EV. 2019. Shaping ethylene response: the role of EIN3/EIL1 transcription factors. *Frontiers in Plant Science* **10**: 1030.

Douglas RN, Wiley D, Sarkar A, Springer N, Timmermans MCP, Scanlon MJ. 2010. Ragged seedling2 encodes an ARGONAUTE7-like protein required for mediolateral expansion, but not dorsiventrality, of maize leaves. *Plant Cell* **22**: 1441–1451.

Etemadi M, Gutjahr C, Couzigou J-M, Zouine M, Lauressergues D, Timmers A, Audran C, Bouzayen M, Becard G, Combier J-P. 2014. Auxin perception is required for arbuscule development in arbuscular mycorrhizal symbiosis. *Plant Physiology* **166**: 281–292.

Fang X, Qi Y. 2016. RNAi in plants: an Argonaute-centered view. *Plant Cell* **28**: 272–285.

Floss DS, Levy JG, Lévesque-Tremblay V, Pumplin N, Harrison MJ. 2013. DELLA proteins regulate arbuscule formation in arbuscular mycorrhizal symbiosis. *Proceedings of the National Academy of Sciences, USA* **110**: E5025–E5034.

Fonouni-Farde C, Diet A, Frugier F. 2016. Root development and endosymbioses: DELLAs lead the orchestra. *Trends in Plant Science* **21**: 898–900.

Foo E, McAdam EL, Weller JL, Reid JB. 2016. Interactions between ethylene, gibberellins, and brassinosteroids in the development of rhizobial and mycorrhizal symbioses of pea. *Journal of Experimental Botany* **67**: 2413–2424.

Foo E, Ross JJ, Jones WT, Reid JB. 2013. Plant hormones in arbuscular mycorrhizal symbioses: an emerging role for gibberellins. *Annals of Botany* **111**: 769–779.

Fracetto GGM, Peres LEP, Lambais MR. 2017. Gene expression analyses in tomato near isogenic lines provide evidence for ethylene and abscisic acid biosynthesis fine-tuning during arbuscular mycorrhiza development. *Archives of Microbiology* **199**: 787–798.

Fujii H, Chiou T, Lin S, Aung K, Zhu J. 2005. A miRNA involved in phosphate-starvation response in Arabidopsis. *Current Biology* **15**: 2038–2043.

Groten K, Nawaz A, Nguyen NHT, Santhanam R, Baldwin IT. 2015. Silencing a key gene of the common symbiosis pathway in *Nicotiana attenuata* specifically impairs arbuscular mycorrhizal infection without influencing the root-associated microbiome or plant growth. *Plant, Cell & Environment* **38**: 2398–2416.

Gu M, Xu K, Chen A, Zhu Y, Tang G, Xu G. 2010. Expression analysis suggests potential roles of microRNAs for phosphate and arbuscular mycorrhizal signaling in *Solanum lycopersicum*. *Physiologia Plantarum* **138**: 226–237.

Gutjahr C. 2014. Phytohormone signaling in arbuscular mycorhiza development. *Current Opinion in Plant Biology* **20**: 26–34.

Gutjahr C, Casieri L, Paszkowski U. 2009. Glomus intraradices induces changes in root system architecture of rice independently of common symbiosis signaling. *New Phytologist* **182**: 829–837.

Halitschke R, Gase K, Hui DQ, Schmidt DD, Baldwin IT. 2003. Molecular interactions between the specialist herbivore *Manduca sexta* (Lepidoptera, Sphingidae) and its natural host *Nicotiana attenuata*. VI. Microarray analysis reveals that most herbivore-specific transcriptional changes are mediated by fatty acid-amino acid conjugates. *Plant Physiology* **131**: 1894–1902.

Heck C, Kuhn H, Heidt S, Walter S, Rieger N, Requena N. 2016. Symbiotic Fungi control plant root cortex development through the novel GRAS transcription factor MIG1. *Current Biology* **26**: 2770–2778.

Hobecker KV, Reynoso MA, Bustos-Sanmamed P, Wen J, Mysore KS, Crespi M, Blanco FA, Zanetti ME. 2017. The microRNA390/TAS3 pathway mediates symbiotic nodulation and lateral root growth. *Plant Physiology* **174**: 2469–2486.

Holt DB, Gupta V, Meyer D, Abel NB, Andersen SU, Stougaard J, Markmann K. 2015. micro RNA 172 (miR172) signals epidermal infection and is expressed in cells primed for bacterial invasion in *Lotus japonicus* roots and nodules. *New Phytologist* **208**: 241–256.

Hsieh L-C, Lin S-I, Shih AC-C, Chen J-W, Lin W-Y, Tseng C-Y, Li W-H, Chiou T-J. 2009. Uncovering small RNA-mediated responses to phosphate deficiency in Arabidopsis by deep sequencing. *Plant Physiology* **151**: 2120–2132.

Hunter C, Sun H, Poethig RS. 2003. The *Arabidopsis* heterochronic gene *ZIPPY* is an *ARGONAUTE* family member. *Current Biology* **13**: 1734–1739.

Johnson NC, Graham JH, Smith FA. 1997. Functioning of mycorrhizal associations along the mutualism-parasitism continuum. *New Phytologist* **135**: 575–586.

Jouannet V, Moreno AB, Elmayan T, Vaucheret H, Crespi MD, Maizel A. 2012. Cytoplasmic Arabidopsis AGO7 accumulates in membrane-associated siRNA bodies and is required for ta-siRNA biogenesis. *EMBO Journal* **31**: 1704–1713.

Keymer A, Pimprikar P, Wewer V, Huber C, Brands M, Bucerius SL, Delaux P-M, Klingl V, Röpenack-Lahaye EV, Wang TL *et al.* 2017. Lipid transfer from plants to arbuscular mycorrhiza fungi. *eLife* **6**: e29107.

Kistner C, Matamoros M. 2005. RNA isolation using phase extraction and LiCl precipitation. In: Márquez AJ, Stougaard J, Udvardi M, Parniske M, Spaink H, Saalbach G, Webb J, Chiurazzi M, Márquez AJ, eds. *Lotus japonicus handbook*. Dordrecht, the Netherlands: Springer, 123–124.

Krügel T, Lim M, Gase K, Halitschke R, Baldwin IT. 2002. *Agrobacterium*-mediated transformation of *Nicotiana attenuata*, a model ecological expression system. *Chemoecology* **12**: 177–183.

Kuo H-F, Chiou T-J. 2011. The role of microRNAs in phosphorus deficiency signaling. *Plant Physiology* **156**: 1016–1024.

Lei K, Lin Y, Ren J, Bai L, Miao Y, An G, Song C. 2015. Modulation of the Phosphate-deficient Responses by the microRNA156 and its targeted SQUAMOSA PROMOTER BINDING PROTEIN-LIKE 3 in Arabidopsis. *Plant and Cell Physiology* **57**: 192–203.

Liao D, Wang S, Cui M, Liu J, Chen A, Xu G. 2018. Phytohormones regulate the development of arbuscular mycorrhizal symbiosis. *International Journal of Molecular Sciences* **19**: 3146.

Lu Y, Feng Z, Liu X, Bian L, Xie H, Zhang C, Mysore KS, Liang J. 2018. MiR393 and miR390 synergistically regulate lateral root growth in rice under different conditions. *BMC Plant Biology* **18**: 261.

Luginbuehl LH, Menard GN, Kurup S, Van Erp H, Radhakrishnan GV, Breakspear A, Oldroyd GED, Eastmond PJ. 2017. Fatty acids in arbuscular mycorrhizal fungi are synthesized by the host plant. *Science* **356**: 1175–1178.

Manavella PA, Yang SW, Palatnik J. 2019. Keep calm and carry on: miRNA biogenesis under stress. *The Plant Journal* **99**: 832–843.

Martín-Rodríguez J, León-Morcillo R, Vierheilig H, Ocampo JA, Ludwig-Müller J, García-Garrido JM. 2011. Ethylene-dependent/ethylene-independent ABA regulation of tomato plants colonized by arbuscular mycorrhiza fungi. *New Phytologist* **190**: 193–205.

Martín-Rodríguez J, Ocampo JA, Molinero-Rosales N, Tarkowská D, Ruíz-Rivero O, García-Garrido JM. 2015. Role of gibberellins during arbuscular mycorrhizal formation in tomato: new insights revealed by endogenous

quantification and genetic analysis of their metabolism in mycorrhizal roots. *Physiologia Plantarum* **154**: 66–81.

McGonigle TP, Evans DG, Miller MH. 1990. Effect of degree of soil disturbance on mycorrhizal colonization and phosphorus absorption by maize in growth chamber and field experiments. *New Phytologist* **116**: 629–636.

Meister G. 2013. Argonaute proteins: functional insights and emerging roles. *Nature Reviews Genetics* **14**: 447–459.

Montgomery TA, Howell MD, Cuperus JT, Li D, Hansen JE, Alexander AL, Chapman EJ, Fahlgren N, Allen E, Carrington JC. 2008. Specificity of ARGONAUTE7-miR390 interaction and dual functionality in TAS3 trans-acting siRNA formation. *Cell* **133**: 128–141.

Morandi D, Sagan M, Prado-Vivant E, Duc G. 2000. Influence of genes determining supernodulation on root colonization by the mycorrhizal fungus Glomus mosseae in *Pisum sativum* and *Medicago truncatula* mutants. *Mycorrhiza* **10**: 37–42.

Mukherjee A, Ané J-M. 2011. Germinating spore exudates from arbuscular mycorrhizal fungi: Molecular and developmental responses in plants and their regulation by ethylene. *Molecular Plant–Microbe Interactions* **24**: 260–270.

Müller LM, Flokova K, Schnabel E, Sun X, Fei Z, Frugoli J, Bouwmeester HJ, Harrison MJ. 2019. A CLE-SUNN module regulates strigolactone content and fungal colonization in arbuscular mycorrhiza. *Nature Plants* **5**: 933–939.

Müller LM, Harrison MJ. 2019. Phytohormones, miRNAs, and peptide signals integrate plant phosphorus status with arbuscular mycorrhizal symbiosis. *Current Opinion in Plant Biology* **50**: 132–139.

Nagasaki H, Itoh J-i, Hayashi K, Hibara K-i, Satoh-Nagasawa N, Nosaka M, Mukouhata M, Ashikari M, Kitano H, Matsuoka M *et al.* 2007. The small interfering RNA production pathway is required for shoot meristem initiation in rice. *Proceedings of the National Academy of Sciences, USA* **104**: 14867–14871.

Navarro L, Dunoyer P, Jay F, Arnold B, Dharmasiri N, Estelle M, Voinnet O, Jones JDG. 2006. A plant miRNA contributes to antibacterial resistance by repressing auxin signaling. *Science* **312**: 436–439.

Navarro-Quezada A, Gase K, Singh RK, Pandey SP, Baldwin IT. 2020. *Nicotiana attenuata* genome reveals genes in the molecular machinery behind remarkable adaptive phenotypic plasticity. In: Ivanov NV, Sierro N, Peitsch MC, eds. *The tobacco plant genome*. Cham, Switzerland: Springer International Publishing, 211–229.

Onkokesung N, Gaquerel E, Kotkar H, Kaur H, Baldwin IT, Galis I. 2012. MYB8 controls inducible phenolamide levels by activating three novel hydroxycinnamoyl-coenzyme A:polyamine transferases in *Nicotiana attenuata*. *Plant Physiology* **158**: 389–407.

Pandey P, Wang M, Baldwin IT, Pandey SP, Groten K. 2018. Complex regulation of microRNAs in roots of competitively-grown isogenic *Nicotiana attenuata* plants with different capacities to interact with arbuscular mycorrhizal fungi. *BMC Genomics* **19**: 937.

Pandey SP, Baldwin IT. 2007. RNA-directed RNA polymerase 1 (RdR1) mediates the resistance of *Nicotiana attenuata* to herbivore attack in nature. *The Plant Journal* **50**: 40–53.

Pandey SP, Baldwin IT. 2008. Silencing RNA-directed RNA polymerase 2 increases the susceptibility of *Nicotiana attenuata* to UV in the field and in the glasshouse. *The Plant Journal* **54**: 845–862.

Pandey SP, Gaquerel E, Gase K, Baldwin IT. 2008. RNA-directed RNA polymerase3 from *Nicotiana attenuata* is required for competitive growth in natural environments. *Plant Physiology* **147**: 1212–1224.

Pant BD, Musialak-Lange M, Nuc P, May P, Buhtz A, Kehr J, Walther D, Scheible W-R. 2009. Identification of nutrient-responsive arabidopsis and rapeseed microRNAs by comprehensive real-time polymerase chain reaction profiling and small RNA sequencing. *Plant Physiology* **150**: 1541–1555.

Park H-J, Floss DS, Levesque-Tremblay V, Bravo A, Harrison MJ. 2015. Hyphal branching during arbuscule development requires reduced arbuscular mycorrhiza. *Plant Physiology* **169**: 2774–2788.

Pegler JL, Oultram JMJ, Grof CPL, Eamens AL. 2020. Molecular manipulation of the miR399/*PHO*$_2$ expression module alters the salt stress response of *Arabidopsis thaliana*. *Plants* **10**: 73.

Penmetsa RV, Frugoli JA, Smith LS, Long SR, Cook DR. 2003. Dual genetic pathways controlling nodule number in *Medicago truncatula*. *Plant Physiology* **131**: 998–1008.

Pimprikar P, Gutjahr C. 2018. Transcriptional regulation of arbuscular mycorrhiza development. *Plant and Cell Physiology* **59**: 678–695.

Pradhan M, Pandey P, Baldwin IT, Pandey SP. 2020. Argonaute 4 modulates resistance to *Fusarium brachygibbosum* infection by regulating jasmonic acid signaling. *Plant Physiology* **184**: 1152.

Pradhan M, Pandey P, Gase K, Sharaff M, Singh RK, Sethi A, Baldwin IT, Pandey SP. 2017. Argonaute 8 (AGO8) mediates the elicitation of direct defenses against herbivory. *Plant Physiology* **175**: 927–946.

Pradhan M, Rocha C, Halitschke R, Baldwin IT, Pandey SP. 2021. microRNA390 modulates *Nicotiana attenuata's* tolerance response to *Manduca sexta* herbivory. *Plant Direct* **5**: e350.

Rech SS, Heidt S, Requena N. 2013. A tandem Kunitz protease inhibitor (KPI106)–serine carboxypeptidase (SCP1) controls mycorrhiza establishment and arbuscule development in *Medicago truncatula*. *The Plant Journal* **75**: 711–725.

Santhanam R, Luu VT, Weinhold A, Goldberg J, Oh Y, Baldwin IT. 2015. Native root-associated bacteria rescue a plant from a sudden-wilt disease that emerged during continuous cropping. *Proceedings of the National Academy of Sciences, USA* **112**: E5013–E5020.

Schnabel E, Journet E-P, de Carvalho-Niebel F, Duc G, Frugoli J. 2005. The *Medicago truncatula* SUNN gene encodes a CLV1-like leucine-rich repeat receptor kinase that regulates nodule number and root length. *Plant Molecular Biology* **58**: 809–822.

Schuck S, Weinhold A, Luu VT, Baldwin IT. 2014. Isolating fungal pathogens from a dynamic disease outbreak in a native plant population to establish plant-pathogen bioassays for the ecological model plant *Nicotiana attenuata*. *PLoS ONE* **9**: e102915.

Silvestri A, Fiorilli V, Miozzi L, Accotto GP, Turina M, Lanfranco L. 2019. *In silico* analysis of fungal small RNA accumulation reveals putative plant mRNA targets in the symbiosis between an arbuscular mycorrhizal fungus and its host plant. *BMC Genomics* **20**: 169.

Singh RK, Gase K, Baldwin IT, Pandey SP. 2015. Molecular evolution and diversification of the Argonaute family of proteins in plants. *BMC Plant Biology* **15**: 23.

Singh RK, Pandey SP. 2015. Evolution of structural and functional diversification among plant Argonautes. *Plant Signaling & Behavior* **10**: e1069455.

Smith SE, Smith FA. 2011. Roles of arbuscular mycorrhizas in plant nutrition and growth: new paradigms from cellular to ecosystem scales. *Annual Review of Plant Biology* **62**: 227–250.

Solaiman ZM, Senoo K, Kawaguchi M, Imaizumi-Anraku H, Akao S, Tanaka A, Obata H. 2000. Characterization of mycorrhizas formed by *Glomus* sp. on roots of hypernodulating mutants of *Lotus japonicus*. *Journal of Plant Research* **113**: 443–448.

Song F, He C, Yan X, Bai F, Pan Z, Deng X, Xiao S. 2018. Small RNA profiling reveals involvement of microRNA-mediated gene regulation in response to mycorrhizal symbiosis in *Poncirus trifoliata* L. Raf. *Tree Genetics & Genomes* **14**: 1082494.

Song X, Li Y, Cao X, Qi Y. 2019. MicroRNAs and their regulatory roles in plant–environment interactions. *Annual Review of Plant Biology* **70**: 489–525.

Sunkar R, Kapoor A, Zhu J-K. 2006. Posttranscriptional induction of two Cu/Zn superoxide dismutase genes in Arabidopsis is mediated by downregulation of miR398 and important for oxidative stress tolerance. *Plant Cell* **18**: 2051–2065.

Sunkar R, Li YF, Jagadeeswaran G. 2012. Functions of microRNAs in plant stress responses. *Trends in Plant Science* **17**: 196–203.

Takeda N, Handa Y, Tsuzuki S, Kojima M, Sakakibara H, Kawaguchi M. 2015. Gibberellin regulates infection and colonization of host roots by arbuscular mycorrhizal fungi. *Plant Signaling & Behavior* **10**: e1028706.

Tominaga T, Miura C, Takeda N, Kanno Y, Takemura Y, Seo M, Yamato M, Kaminaka H. 2019. Gibberellin promotes fungal entry and colonization during paris-type arbuscular mycorrhizal symbiosis in *Eustoma grandiflorum*. *Plant and Cell Physiology* **61**: 565–575.

Torres de los Santos R, Molinero Rosales N, Ocampo JA, García-Garrido JM. 2016. Ethylene alleviates the suppressive effect of phosphate on arbuscular mycorrhiza formation. *Journal of Plant Growth Regulation* **35**: 611–617.

Trouvelot A, Kough JL, Gianinazzi-Pearson V. 1986. Mesure du taux de mycorhization VA d'un système radiculaire. Recherche de méthode d'estimation ayant une signification fonctionnelle. In: Gianinazzi-Pearson V,

Gianinazzi S, eds. *Physiological and genetical aspects of mycorrhizae: proceedings of the 1st European Symposium on Mycorrhizae, DIJON, 1–5 July 1985*. Paris, France: INRA, 217–221.

Vidal EA, Araus V, Lu C, Parry G, Green PJ, Coruzzi GM, Gutiérrez RA. 2010. Nitrate-responsive miR393/AFB3 regulatory module controls root system architecture in *Arabidopsis thaliana*. *Proceedings of the National Academy of Sciences, USA* **107**: 4477–4482.

Voß S, Betz R, Heidt S, Corradi N, Requena N. 2018. RiCRN1, a crinkler effector from the Arbuscular mycorrhizal fungus Rhizophagus irregularis, functions in arbuscule development. *Frontiers in Microbiology* **9**: 2068.

Wang C, Reid JB, Foo E. 2018. The art of self-control – autoregulation of plant–microbe symbioses. *Frontiers in Plant Science* **9**: 988.

Wang H, Chua NH. 2014. Big effects of small RNAs on legume root biotic interactions. *Genome Biology* **15**: 475.

Wang M, Schäfer M, Li D, Halitschke R, Dong C, McGale E, Paetz C, Song Y, Li S, Dong J *et al.* 2018a. Blumenols as shoot markers of root symbiosis with arbuscular mycorrhizal fungi. *eLife* **7**: e37093.

Wang M, Wilde J, Baldwin IT, Groten K. 2018b. *Nicotiana attenuata's* capacity to interact with arbuscular mycorrhiza alters its competitive ability and elicits major changes in the leaf transcriptome. *Journal of Integrative Plant Biology* **60**: 242–261.

Wu G, Park MY, Conway SR, Wang J-W, Weigel D, Poethig RS. 2009. The sequential action of miR156 and miR172 regulates developmental timing in Arabidopsis. *Cell* **138**: 750–759.

Wu P, Wu Y, Liu C-C, Liu L-W, Ma F-F, Wu X-Y, Wu M, Hang Y-Y, Chen J-Q, Shao Z-Q *et al.* 2016. Identification of Arbuscular Mycorrhiza (AM) – responsive microRNAs in tomato. *Frontiers in Plant Science* **7**: 429.

Xie X, Lai W, Che X, Wang S, Ren Y, Hu W, Chen H, Tang M. 2022. A SPX domain-containing phosphate transporter from Rhizophagus irregularis handles phosphate homeostasis at symbiotic interface of arbuscular mycorrhizas. *New Phytologist* **234**: 650–671.

Xu L, Yang L, Pi L, Liu Q, Ling Q, Wang H, Poethig RS, Huang H. 2006. Genetic interaction between the AS1–AS2 and RDR6–SGS3–AGO7 pathways for leaf morphogenesis. *Plant and Cell Physiology* **47**: 853–863.

Xu M, Hu T, Zhao J, Park M-Y, Earley KW, Wu G, Yang L, Poethig RS. 2016. Developmental functions of miR156-regulated SQUAMOSA PROMOTER BINDING PROTEIN-LIKE (SPL) genes in *Arabidopsis thaliana*. *PLoS Genetics* **12**: e1006263.

Yin H, Hong G, Li L, Zhang X, Kong Y, Sun Z, Li J, Chen J, He Y. 2019. miR156/SPL9 regulates reactive oxygen species accumulation and immune response in *Arabidopsis thaliana*. *Phytopathology* **109**: 632–642.

Yu N, Luo D, Zhang X, Liu J, Wang W, Jin Y, Dong W, Liu J, Liu H, Yang W *et al.* 2014. A DELLA protein complex controls the arbuscular mycorrhizal symbiosis in plants. *Cell Research* **24**: 130–133.

Yu N, Niu Q-W, Ng K-H, Chua N-H. 2015. The role of miR156/SPLs modules in Arabidopsis lateral root development. *The Plant Journal* **83**: 673–685.

Zhang QQ, Wang JG, Wang LY, Wang J, Wang Q, Yu P, Bai MY, Fan M. 2019. Gibberellin repression of axillary bud formation in Arabidopsis by modulation of DELLA-SPL9 complex activity. *Journal of Integrative Plant Biology* **62**: 421–432.

Zhu C, Ding Y, Liu H. 2011. MiR398 and plant stress responses. *Physiologia Plantarum* **143**: 1–9.

Supporting Information

Additional Supporting Information may be found online in the Supporting Information section at the end of the article.

Fig. S1 Evaluation of irAGO7 plants grown in the field.

Fig. S2 Glasshouse studies suggest that ir*AGO7* and WT plants have similar rosette leaf numbers, chlorophyll contents, as well as roots (root length or lateral root numbers).

Fig. S3 Silencing *AGO7* does not affect plant growth and fitness when grown under non-competitive, P-limited conditions with AMF ($n = 10$), or competitive, P-limited conditions without AMF ($n = 6$).

Fig. S4 Silencing *AGO1*, *2*, *4*, or *10* does not affect competitive plant fitness or AMF colonization rates in *Nicotiana attenuata* in competitive P-limited conditions identical to those in Figs 2(c) and 3.

Fig. S5 Microscopic examination of AMF-colonized roots of WT and irAGO7 plants with the help of WGA-fluorescein staining.

Fig. S6 Transcript abundances of transporter genes relevant for a functional plant–AMF interaction.

Fig. S7 miRNA accumulation in WT and irAGO7 roots at the time of AMF inoculation (t_0) using quantitative real-time PCR assays.

Fig. S8 Temporal dynamics of miRNA accumulation in WT and ir*AGO7* roots during AMF colonization using quantitative real-time PCR (qPCR) analysis.

Fig. S9 Elicitation dynamics of putative target genes in AMF inoculated roots of WT and ir*AGO7*. Transcripts of ECI gene were used as internal control for normalization.

Fig. S10 Transformation vector maps for overexpression of 7 miRNAs for determining their function in plant–AMF interaction.

Fig. S11 Evaluation of shoot and root biomass of *Nicotiana attenuata* plants overexpressing 7 miRNAs compared to the EV counterparts.

Fig. S12 Phenotypic characterization of plants overexpressing miR473 and PN-59 in the absence of AMF.

Methods S1 Detailed description of the materials and the methods used in this study.

Table S1 List of primers (of genes and of miRNAs) used in this study.

Table S2 Details of miRNA overexpression construct.

Table S3 Statistical details of parameters tested in Fig. 6.

Please note: Wiley is not responsible for the content or functionality of any Supporting Information supplied by the authors. Any queries (other than missing material) should be directed to the *New Phytologist* Central Office.